Introduction to Neutron Imaging

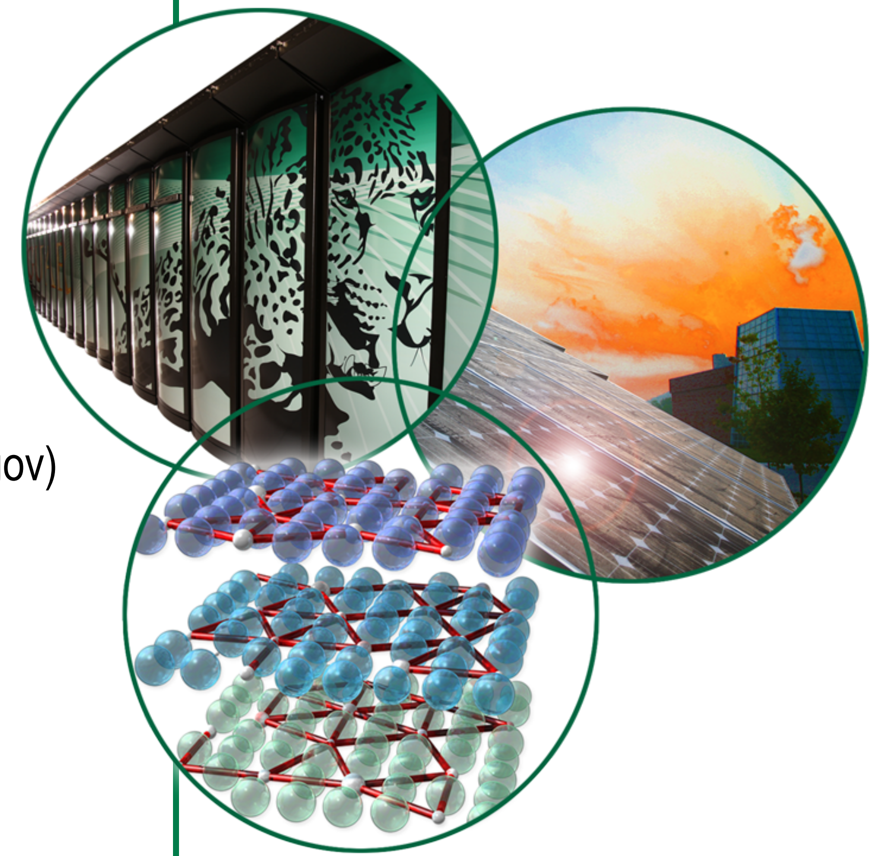

Neutron Imaging Team

Hassina Bilheux, Instrument Scientist (bilheuxhn@ornl.gov)
Jean Bilheux, Computer Scientist
Lakeisha Walker, Scientific Associate
Lou Santodonato, Scientific Associate

Neutrons Measure Structure

Neutron Diffraction

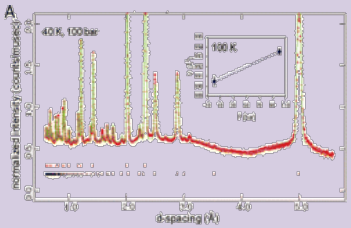

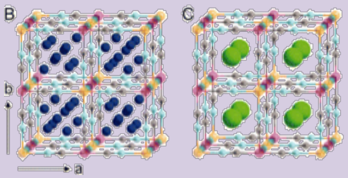

Neutron diffraction of D_2 sorption in $Cu3[Co(CN)_6]_2$

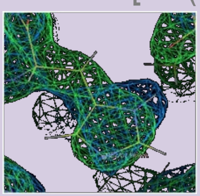

Nuclear and electronic density in enzymes

Neutron Scattering

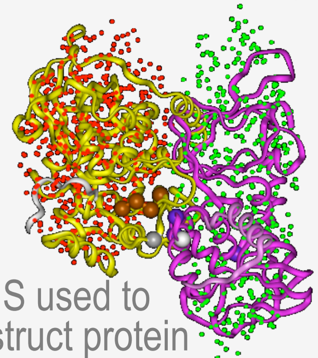

SANS used to construct protein kinase A (PKA)

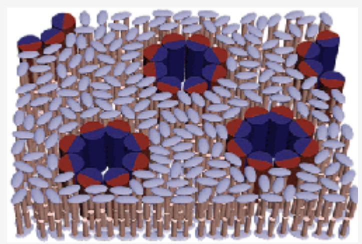

Characterization of biological membranes, colloids, porosity, etc.

Neutron Microscopy

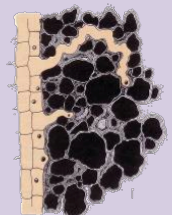

Soil-root interface (rhizosphere)

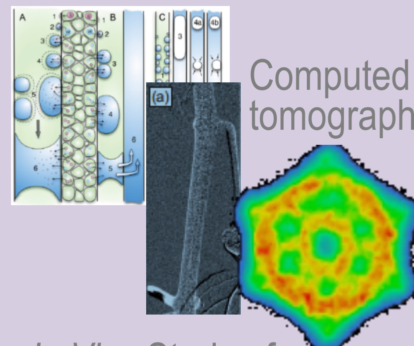

Computed tomography

In Vivo Study of Embolism Formation

Neutron Imaging

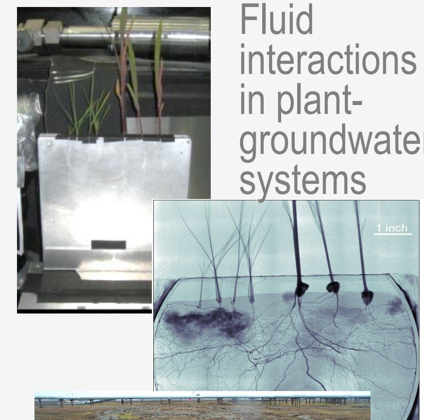

Fluid interactions in plant-groundwater systems

Ice/water segregation in permafrost structures

Inferred structure (indirect) ← → *Direct structure*

10^{-11}	10^{-9}	10^{-7}	10^{-5}	10^{-3}
0.1Å	1.0nm	0.1μm	10.0μm	1mm

Dimension (meters)

What is imaging?

- **Imaging is the visual representation of an object:** photography, cinematography, medical imaging, X-ray imaging, thermal imaging, molecular imaging, neutron imaging, etc.

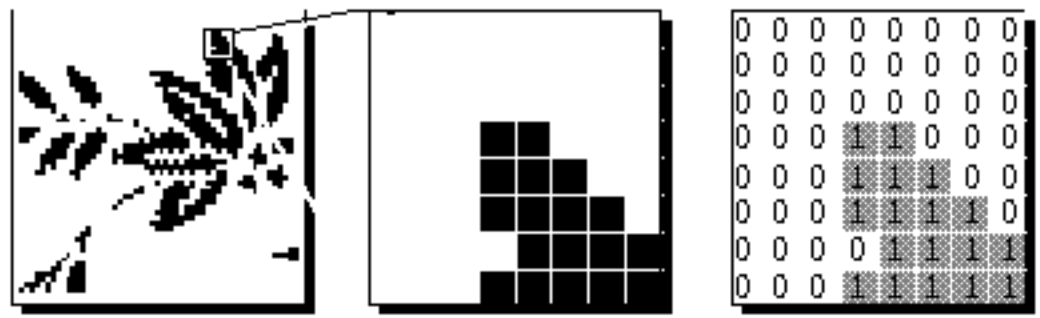

- **Digital Imaging is a field of computer science covering images that can be stored on a computer as *bit-mapped* images**

Imaging throughout Nobel Prize history

- 1901: Roentgen, FIRST Nobel Prize in Physics, Discovery of X-rays
- 1979: Cormack and Hounsfield, Nobel Prize in Medicine, Computed Tomography (CT)
- 1986: Ruska, Binnig, Rohrer, Nobel Prize in Physics, Electron Miscroscopy
- 2003: Lauterbur and Mansfield, Nobel Prize in Medicine, Magnetic Resonance Imaging (MRI)
- 2009: Boyle and Smith, Nobel Prize in Physics, Imaging semi-conductor circuit, the CCD* sensor

- (*) Charge-Coupled Device

Early neutron imaging measurements

- **Neutron Imaging started in the mid 1930's but only during the past 30 years has it come to the forefront of non-destructive testing**

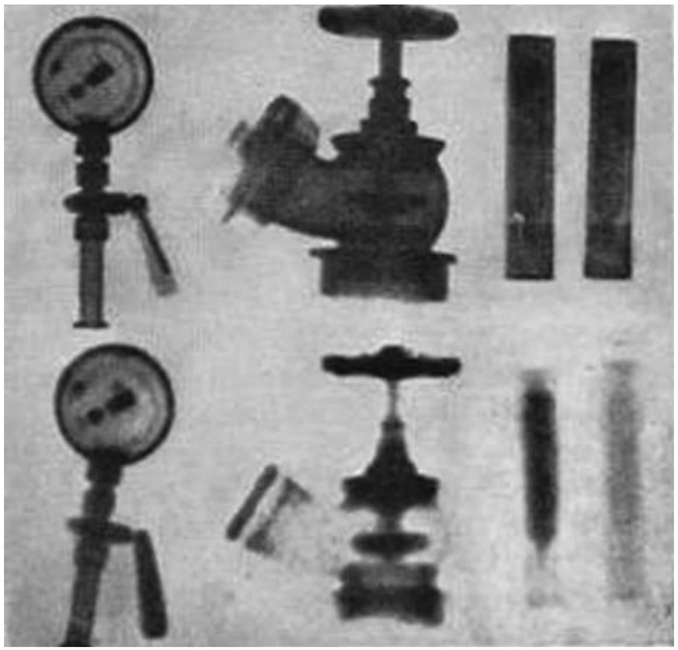

Discovery of neutron in 1932 by Chadwick

First neutron radiograph in 1935

Left to right: Pressure gauge with metal backplate; fire hydrant and test tubes filled with H_2O
and D_2O imaged with gamma-rays (top) and neutrons (bottom)
[Kallman and Kuhn, Research 1, 254 (1947)]

- **World class dedicated imaging user facilities such as NIST, PSI, HZB, FRM-II, J-PARC and at many worldwide universities**
- **World conferences and workshops being held regularly**
- **Growing worldwide user community**

Multiple scattering and low detector spatial resolution

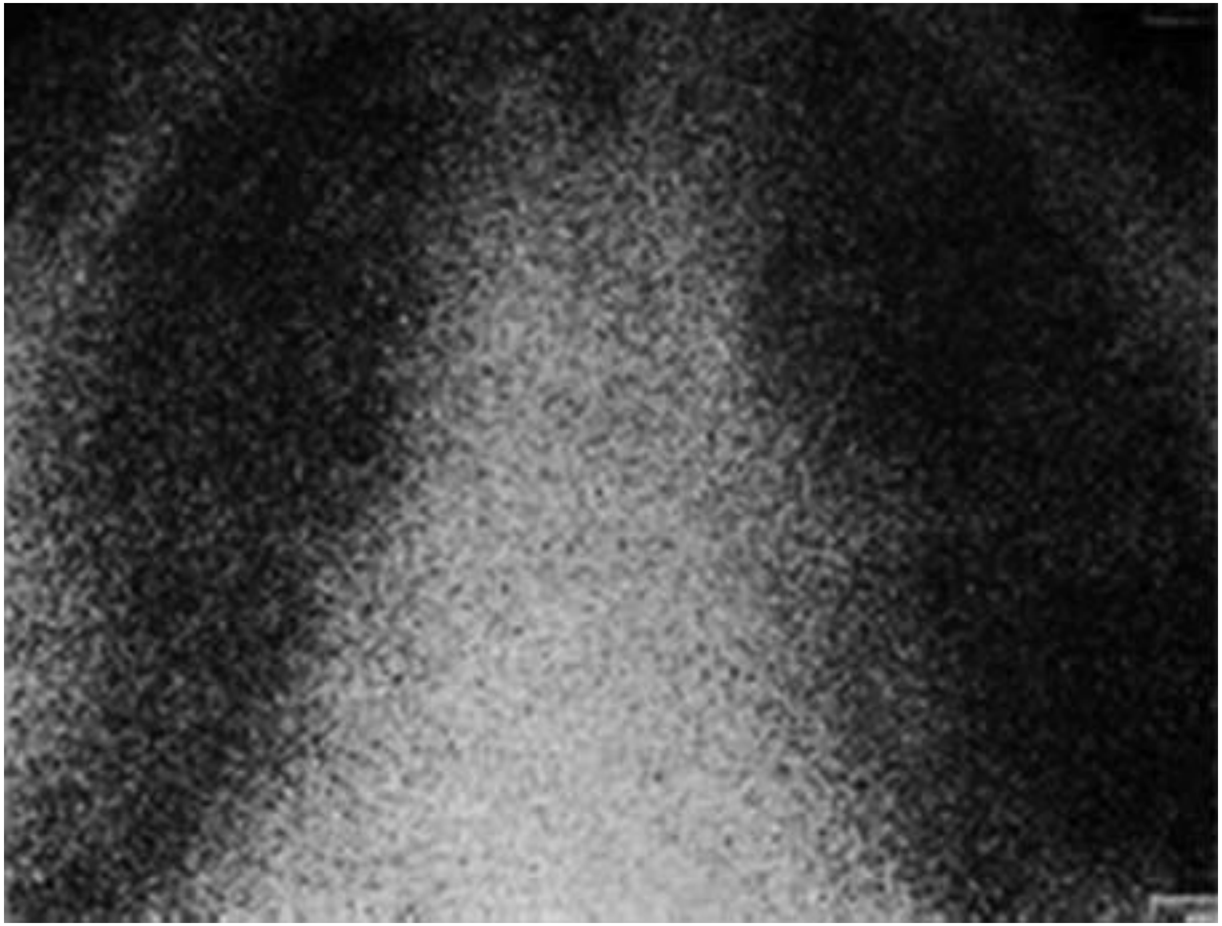

[J. Anderson et al., Br. J. Radiol. 37, 957 (1964)]

Comparison microscopy/microCT and neutron radiography

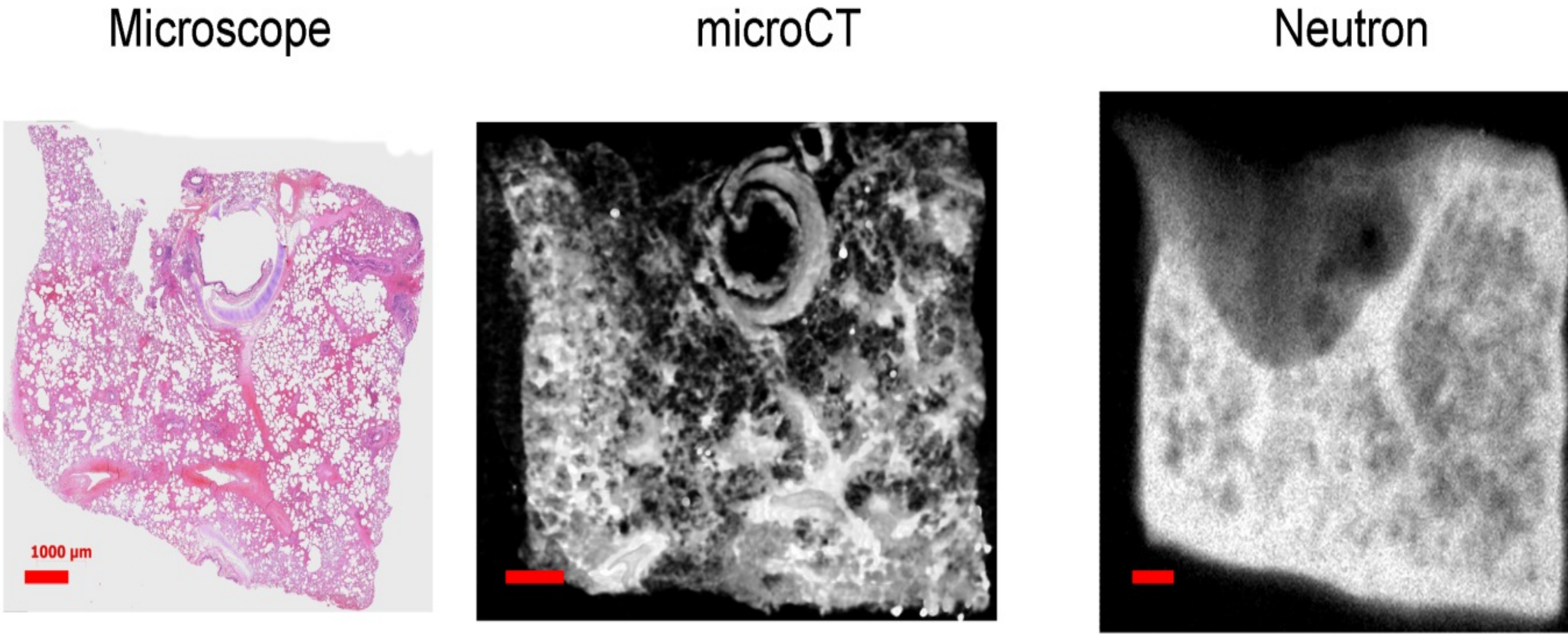

- **92% of the pixel intensities agreement between histological and neutron**

Watkin, K. et al., Neutron Imaging and Applications, Springer, 2009.

Neutron sensitivity

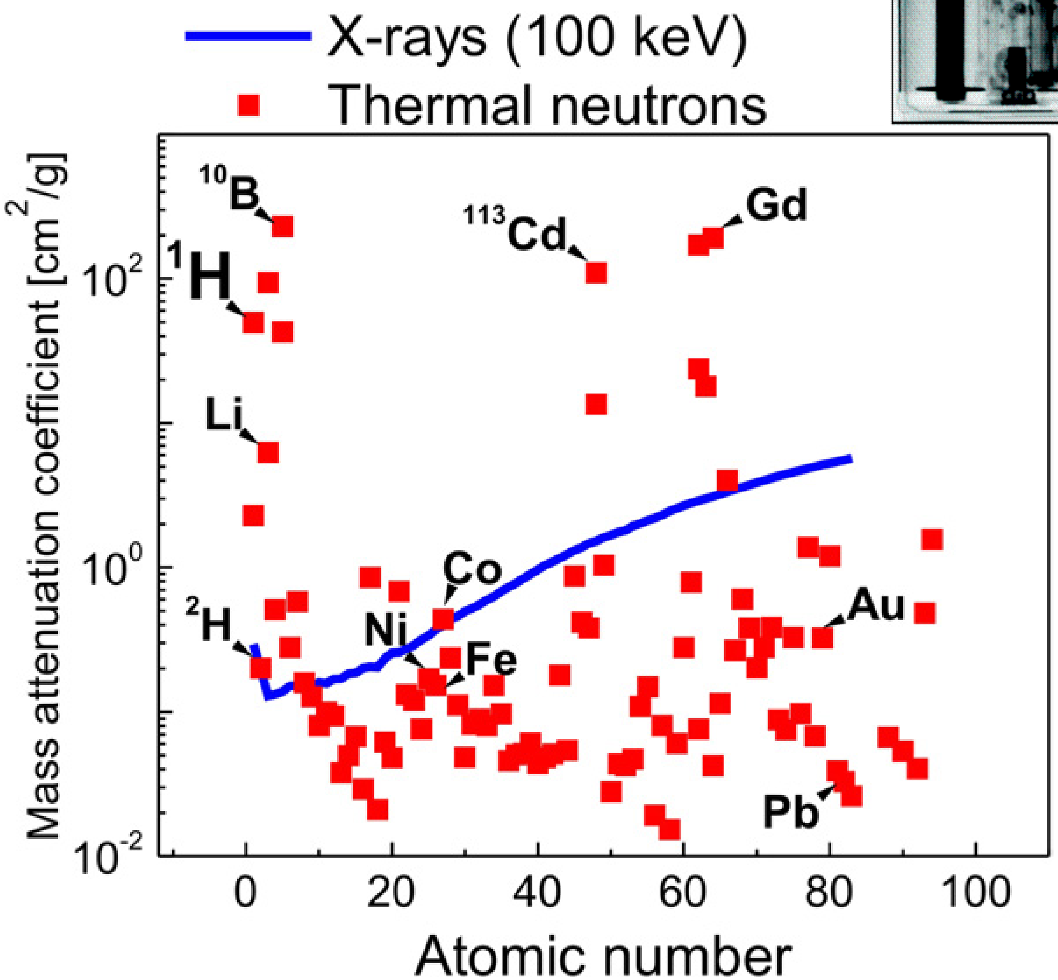

[M. Strobl et al., J. Phys. D: Appl. Phys. **42** (2009) 243001]

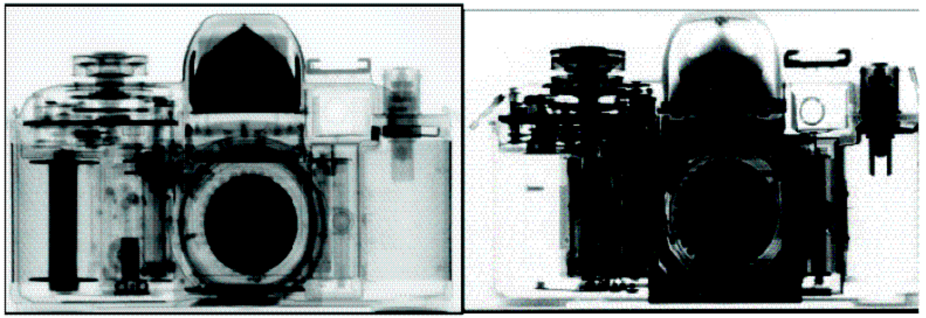

Neutron *Radiograph of camera* ***X-ray*** *Radiograph of camera*

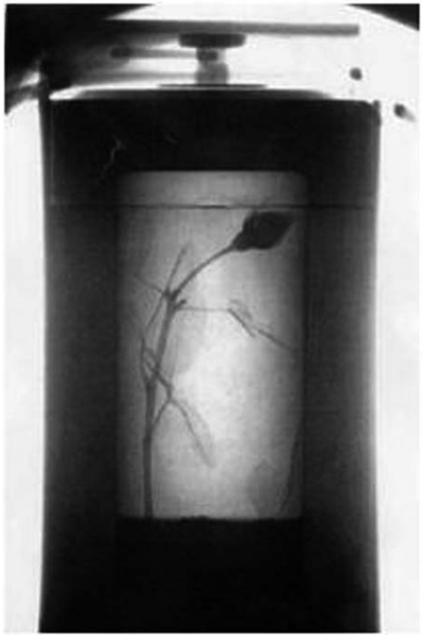

Neutron *Radiograph of Rose in Lead Flask*

Courtesy of E. Lehmann,PSI

Basics of Neutron imaging

Nanda et al., Journal of Physical Chemistry C, 2012.

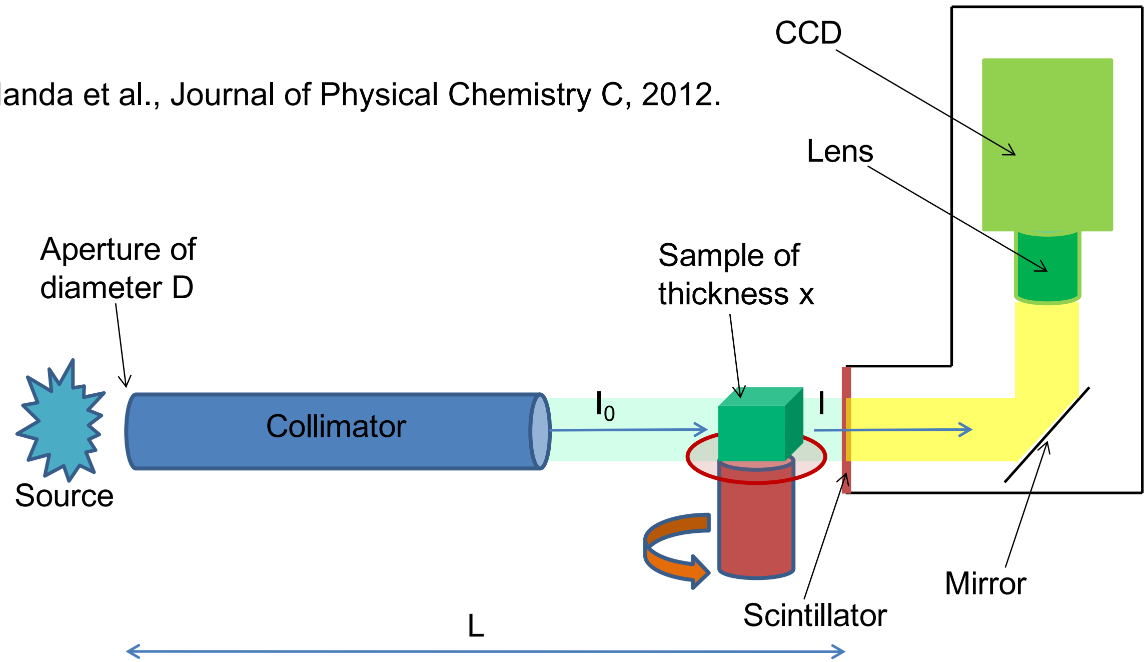

Photograph

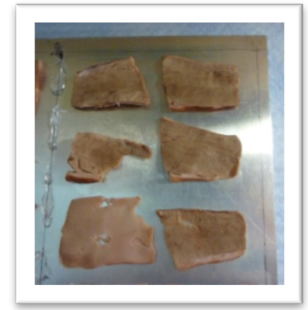

Neutron Radiograph

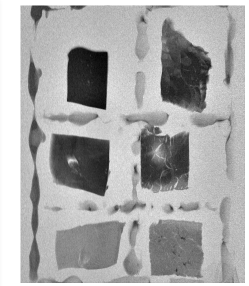

Beam attenuation caused by a **homogeneous uniformly** thick sample composed of a **single isotope** is given by

$$I(\lambda) = I_0(\lambda)e^{-\mu(\lambda)x}$$

$$\mu(\lambda) = \sigma_t(\lambda)\frac{\rho N_A}{M}$$

$\sigma_t(\lambda)$ = scattering and absorption

μ is the attenuation coefficient and Δx is the thickness of the sample

$\sigma_t(\lambda)$ is the material's total cross section for neutrons, ρ is its density, N_A is Avogadro's number, and M is the molar mass.

Detection of “imaging” neutrons

- Scintillator-based techniques such as $^{6}Li(n,\alpha)\,^{3}H$
  - Good signal-to-noise (SNR) ratio
  - Large Field Of View (FOV) and 0.01 to hundreds of seconds images
  - BUT spatial resolution limited by the dissipation of particles
  - Can take a lot of neutron flux!

1,1	1,2	1,3	…	…	1, ny
2,1	2,2	2,3	…	…	2, ny
3,1	3,2	…	…	…	3, ny
…	…	…	…	…	…, nx
nx, 1	nx, 2	nx, 3	…	…	nx, ny

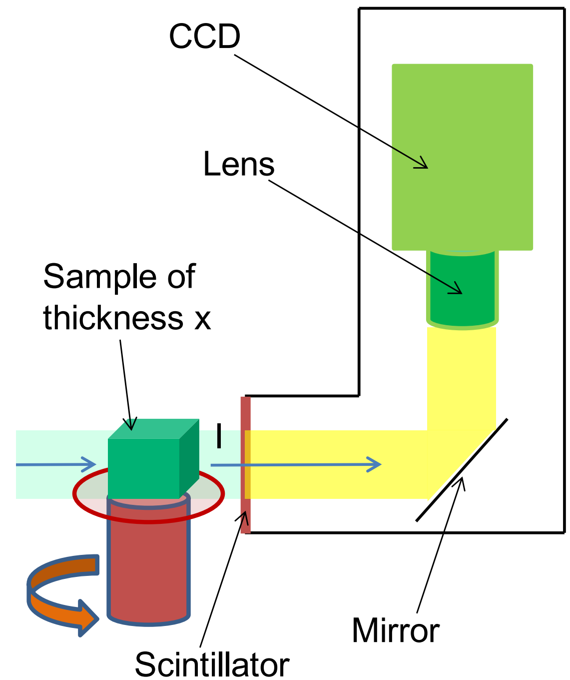

Each pixel is coded using n-bit.
16-bit = pixel value is between 0 and 65535

Detection of "imaging" neutrons (cont'd)

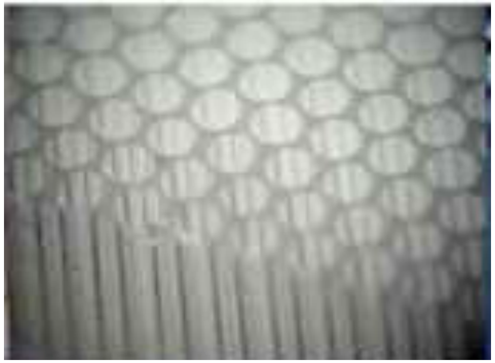

Courtesy of Prof. A. Tremsin, UC-Berkeley

- Pixelated detectors
  - Micro-Channel Plate (MCP)
  - In the direct path of the beam
  - Limited FOV for high spatial resolution MCPs
    - 1.4 cm x 1.4 cm at ~ 15 microns
  - Encodes events at x, y position and time of arrival, at high temporal resolution ~ 1 MHz
  - Detection efficiency has improved for both cold (~70%) and thermal (~50%) energy range
  - Absence of readout noise
  - Not as gamma sensitive
  - Becoming commercial
  - BUT: works in relatively low-signal beam!

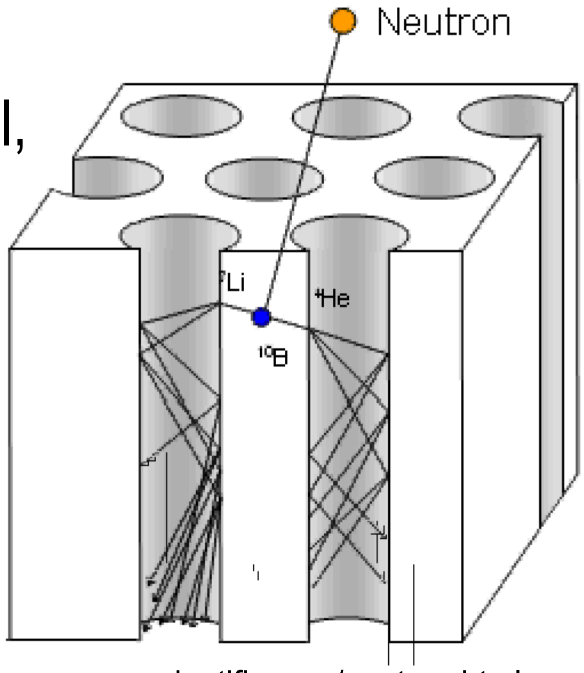

http://www.novascientific.com/neutron.html

Example: Cu, Zn and Al

Compound	Abs. Coeff. [Å^{-2}]	Inc. Coeff. [Å^{-1}]
Cu (100%)	1.78E-09	4.65E-10
Al (100%)	7.75E-11	4.94E-12
Zn (100%)	4.06E-10	5.06E-11

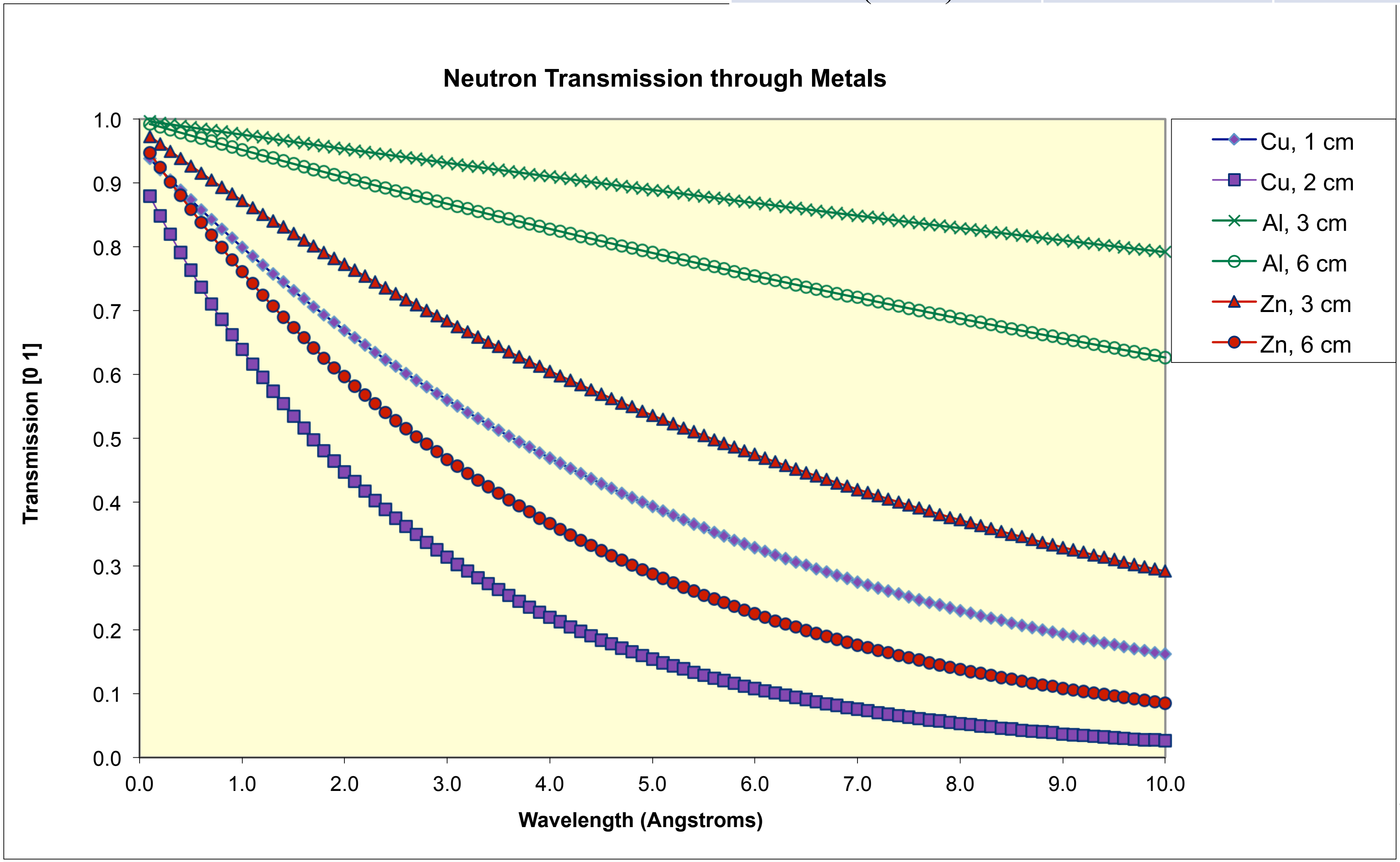

CG1-D: Neutron Imaging Prototype Beamline (Polychromatic/Chopped)

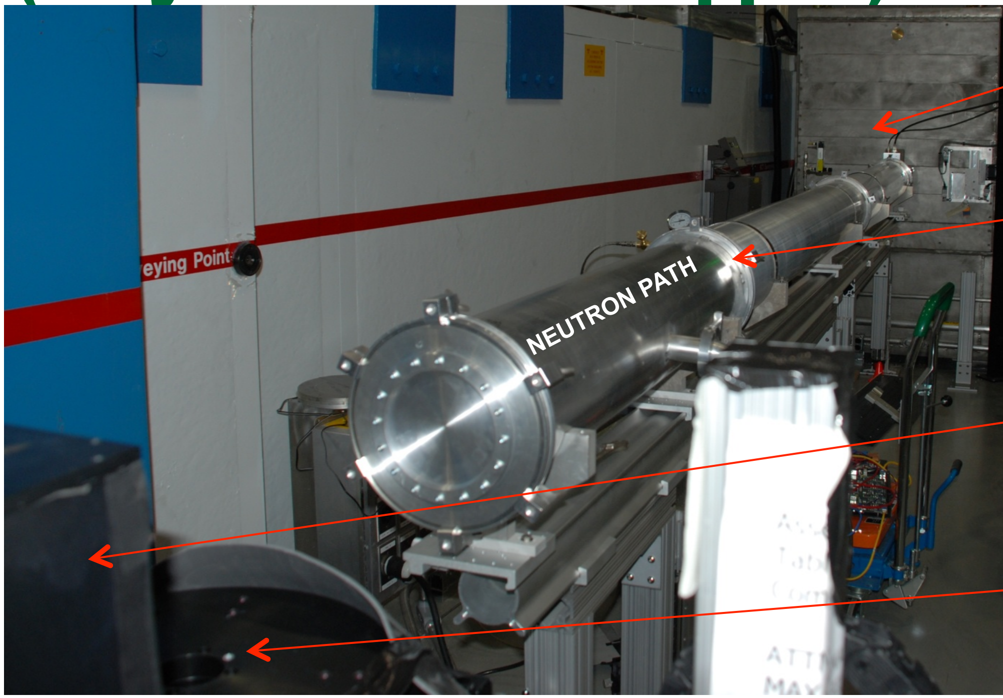

Chopper Box

He-filled Al flight tubes

Detector housing (CCD, lens, mirror and scintillator)

Sample stage (translation and rotation for neutron Computed Tomography)

HFIR CG1D beamline
Current resolution ~ 50 microns

- •ANDOR Camera:
  4Mpixels – 2048x2048
- •Field of view:
  7x7cm^2
- •Quantum Efficiency:
  95%

Al Mirror

Lens

LiF/ZnS scintillator (25 to 200μm thick)

CCD

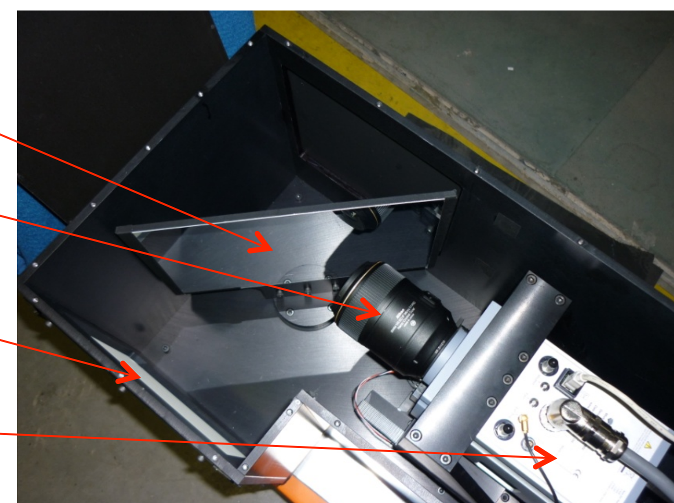

CG-1D Neutron Imaging Facility

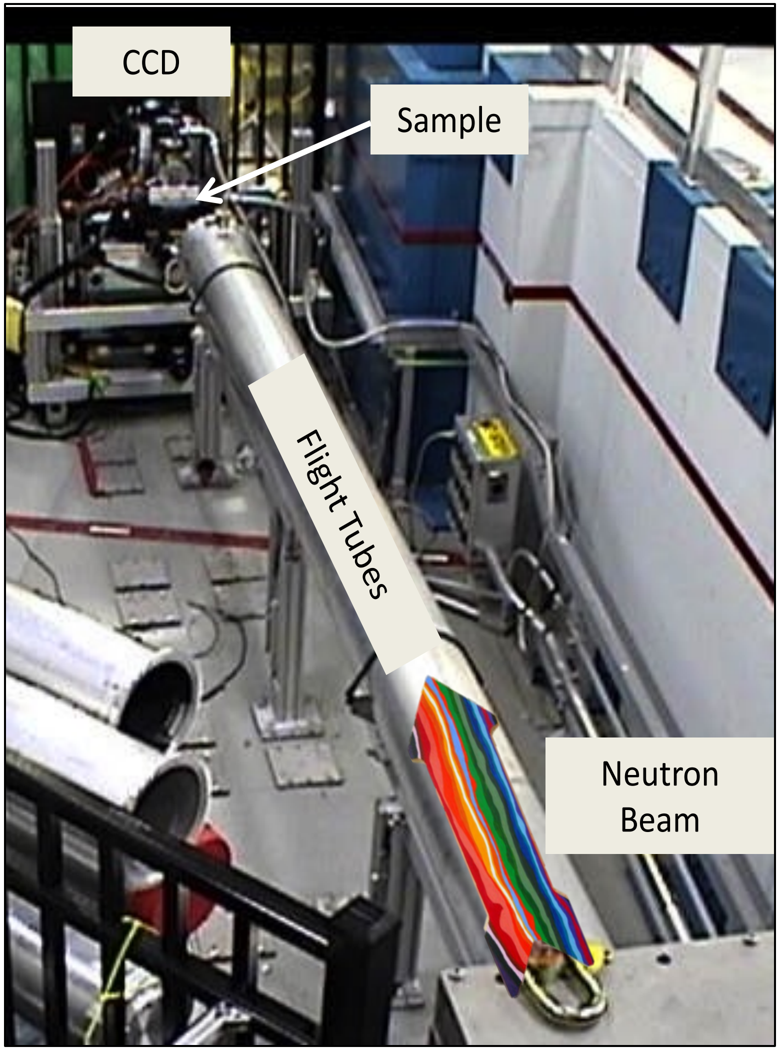

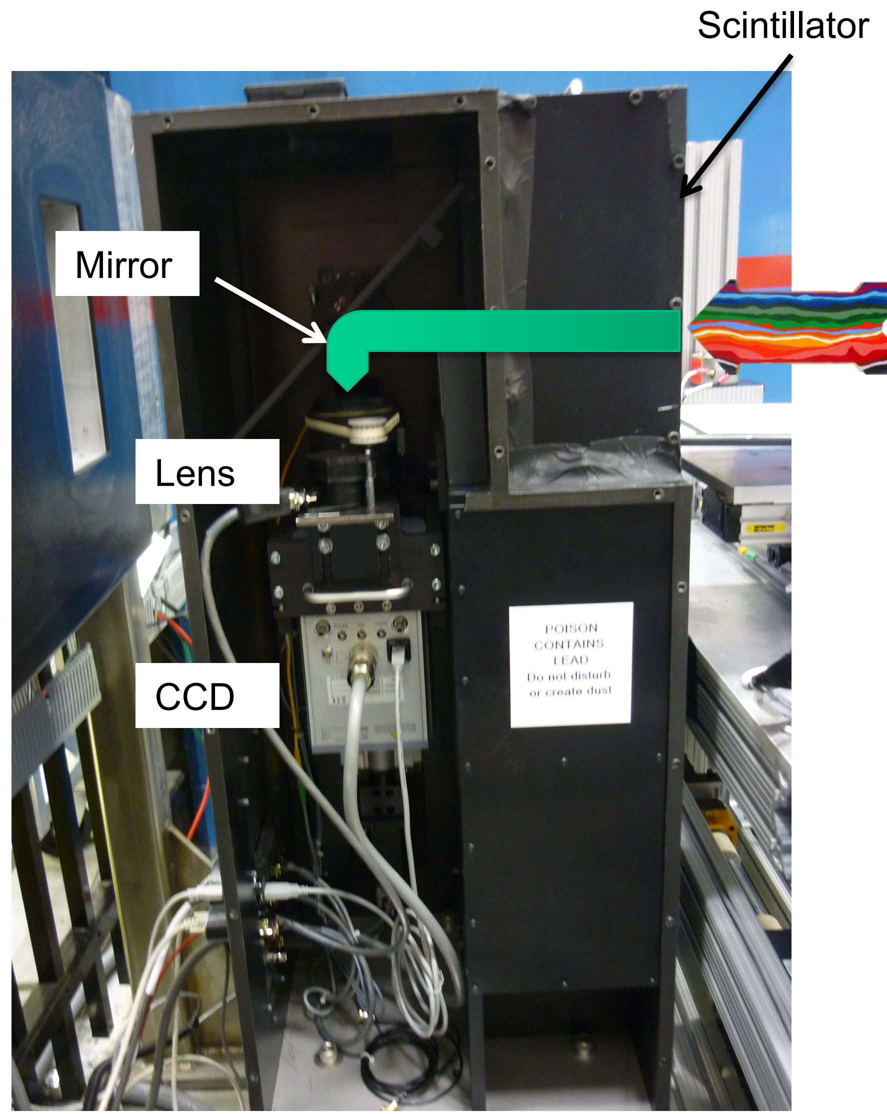

Managed by UT-Battelle
for the U.S. Department of Energy

Use of Diffusers

- 1 cm thick Graphite Powder (4 to 10 microns)

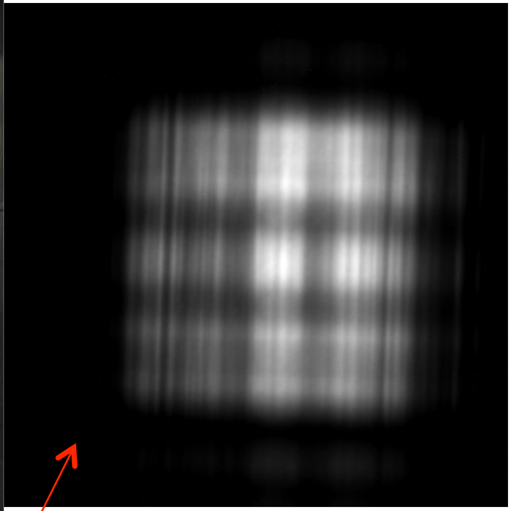

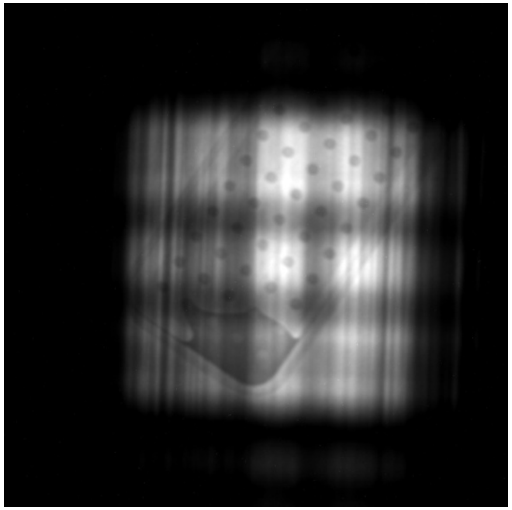

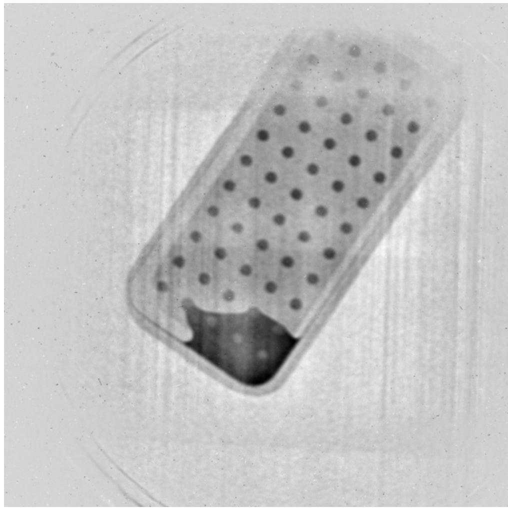

Open Beam

Heat Pipe Sample

Reduced Image

Without diffuser

With diffuser

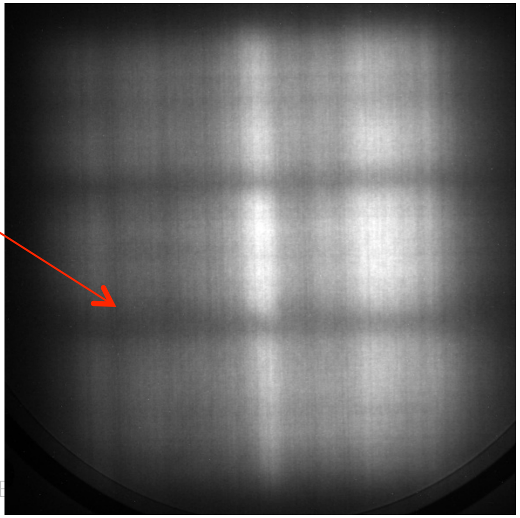

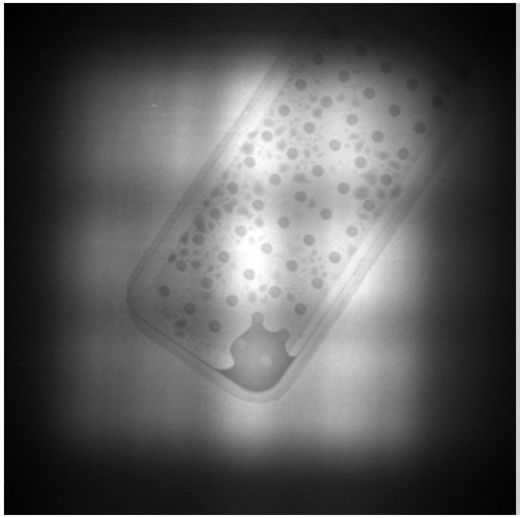

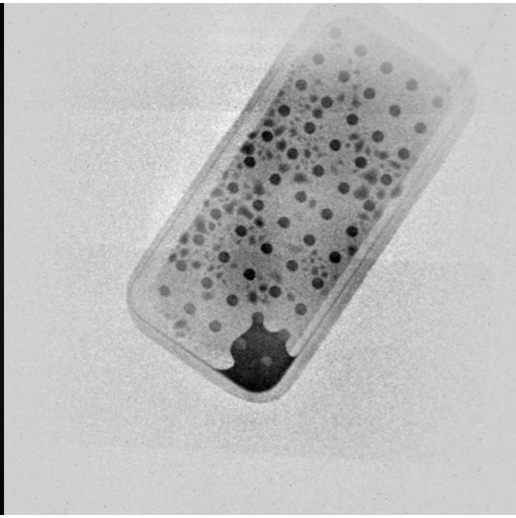

CG-1D polychromatic beam

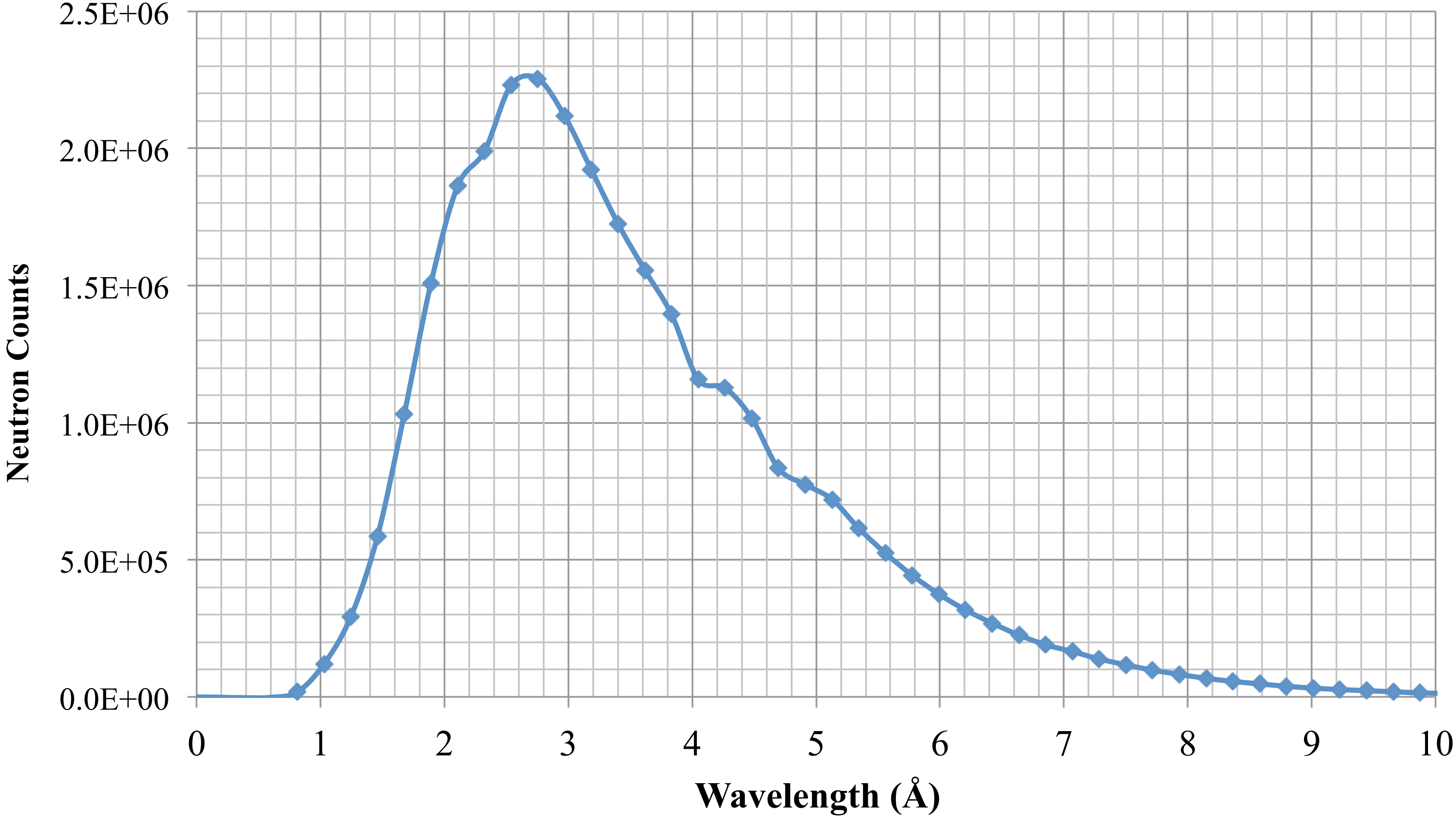

CG-1D spectrum measured with the MCP detector at a flight path distance of approximately 5.5 m, with the chopper running at a frequency 40 Hz and an 5 mm aperture. *[Bilheux et al., ITMNR-7, Canada, June 2012]*

Data Normalization for Imaging

- 2D – Radiography
  - Normalization

$$I_N(i,j) = \frac{I(i,j) - DF(i,j)}{OB(i,j) - DF(i,j)}$$

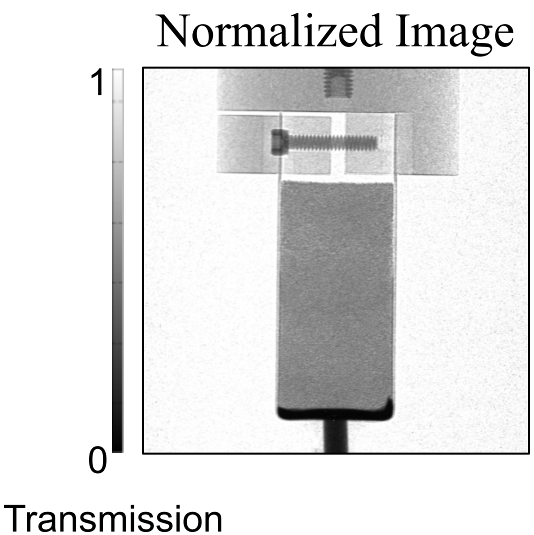

=

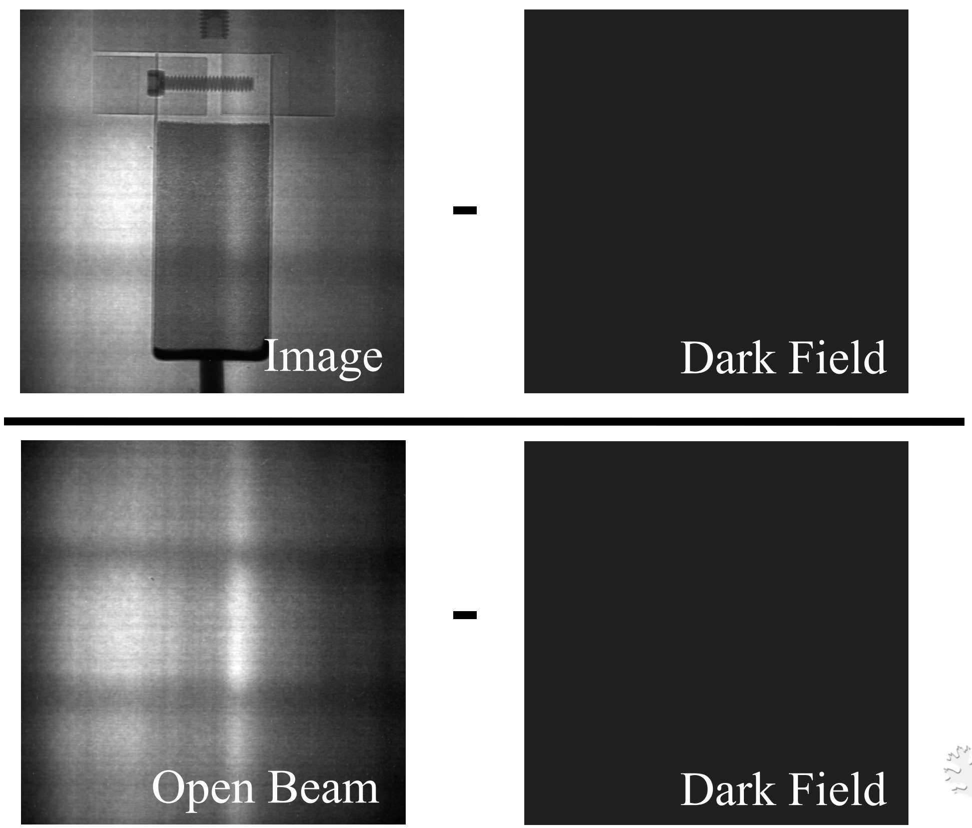

Computed/Computerized Tomography (CT)

- Several techniques:
  - Filtered Back Projection
    - Radon transform
    - Works well with high signal to noise ration measurements
    - Easy-to-use commercial, semi-automated software available
    - Quick
  - Iterative Reconstruction
    - Direct approach
    - Less artifacts
    - Can reconstruct incomplete data
    - High computation time

Computed/Computerized Tomography (FBP)

– **Filtered back projection method**

Raw Data: 2048x2048 pixels, 721 projections → **Normalized Data:** 2048x2048 pixels, 721 projections → **Sinograms:** 2048x721 pixels, 2048 files → **Slices:** 2048x2048 pixels, 2048 slices → **3D reconstruction: 2048x2048x2048 voxels**

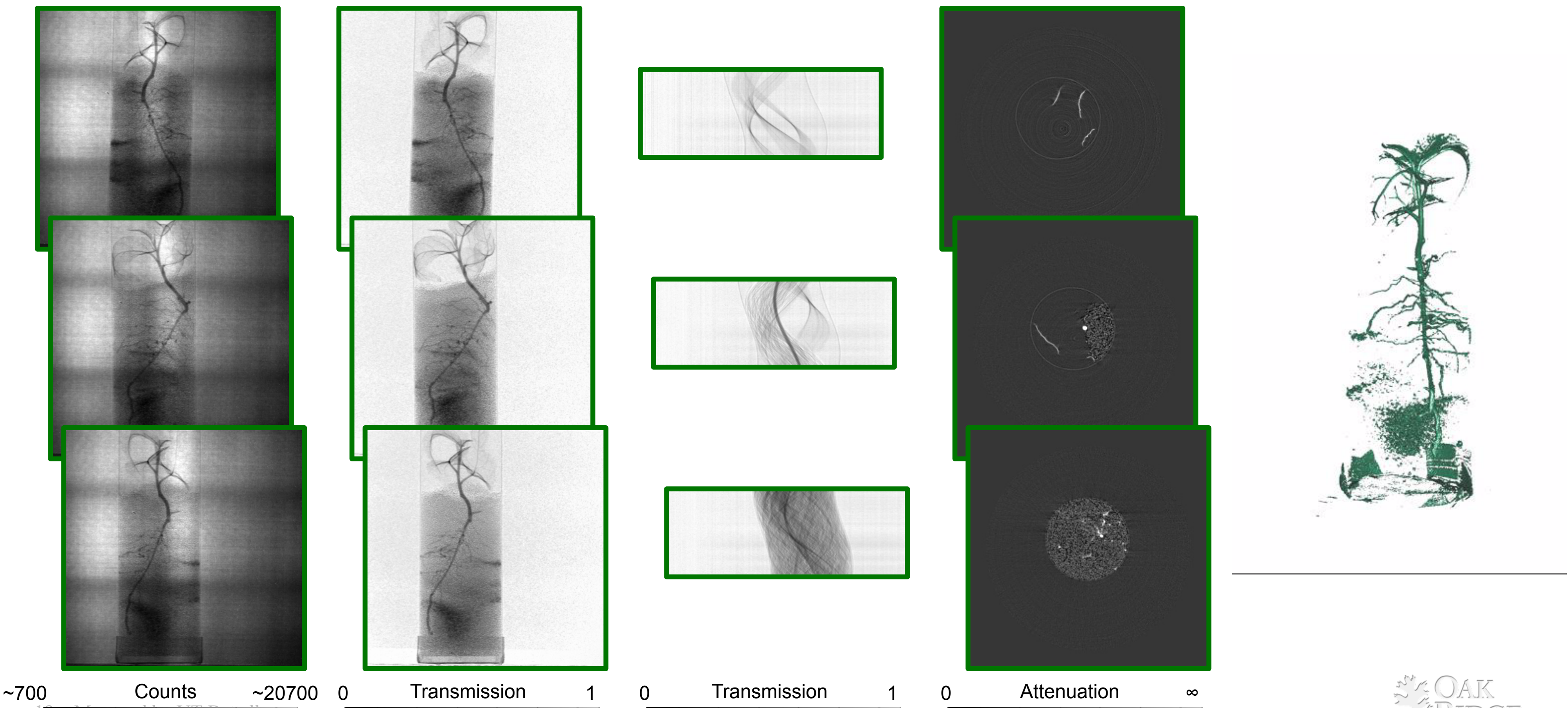

Data reduction and analysis per user request

- **Peformed using iMARS (Neutron Sciences software, Matlab-based) and/or VGStudio (commercial software)**

We develop tools users can utilize to perform their analysis:
-Software engineer interacts with users on a case by case basis
- Calibrated data sets used to test new module

- ✓ Normalization
- ✓ Profiles
- ✓ ROIs
- ✓ Voids and Porosity
- ✓ Segmentation
- ✓ Filters (ISS)

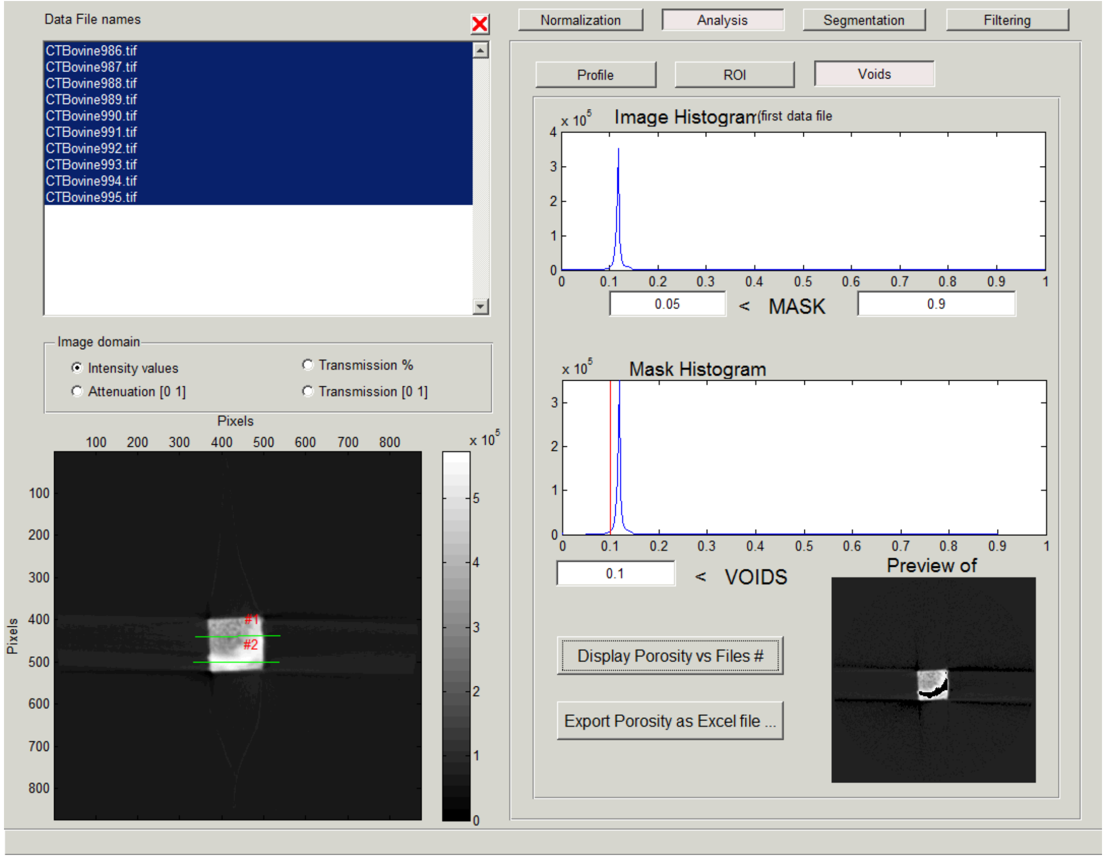

We continue to use VisIt for large data sets (create VTK file using MatLab code).

Data analysis

- Peformed using iMARS (Neutron Sciences software) and/or VGStudio (commercial software)

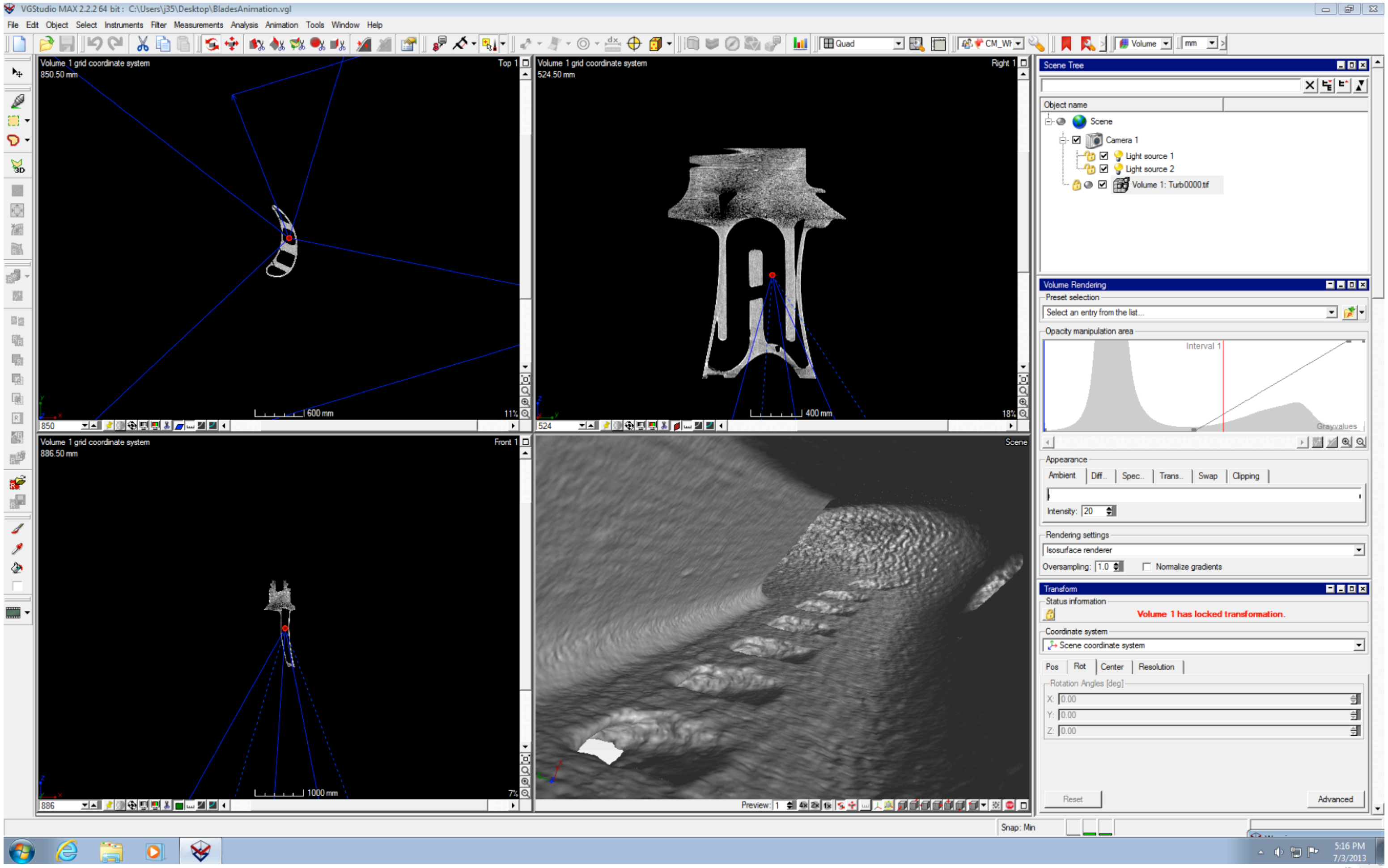

Conventional Neutron Imaging Techniques at steady-state sources

- Radiography (available at CG-1D)
- Tomography (available at CG-1D)
- Phase Contrast Imaging
- Polarized Neutron Imaging
- Stroboscopic Imaging
- Imaging of processes that happen fast
- Energy selective techniques possible with double-monochromator configuration

Neutron Imaging Techniques at pulsed sources

- Energy-selective (or Time-of-Flight) imaging
  - Contrast enhancement
  - Bragg edge
- Stroboscopic imaging
  - SNS has a natural clock
- Neutron Imaging at energies not accessible at reactor facilities
  - Mainly bio-medical applications

Neutron imaging techniques

- Radiography
- Computed tomography
- Bragg edge imaging
- Neutron phase imaging
- Stroboscopic imaging
- Neutron Stimulated Computed Emission Tomography or NSECT
- Polarized imaging
- Dark field imaging
- Energy resonance imaging

Bragg Edge Imaging

- **At reactors:**
  - monochromatic beams
  - Scintillator-based detection adequate
- **At spallation sources:**
  - Time-stamping of neutrons
  - Pixelated detectors such as MCPs required for time measurements

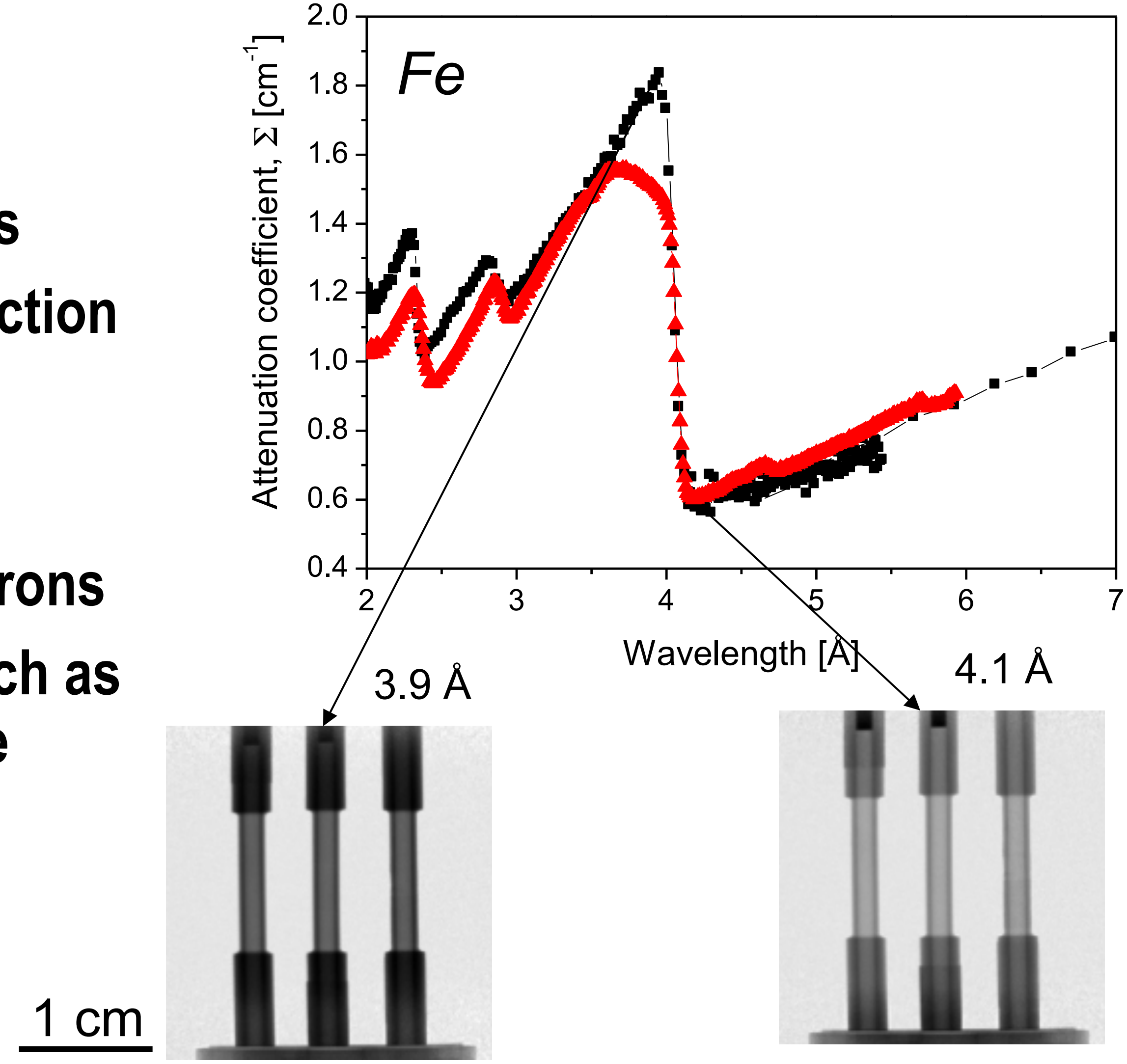

Courtesy of Prof. D. Penumadu, UTK and N. Kardjilov, HZB

Bragg Edge Imaging

- **Strain mapping od steel screw**

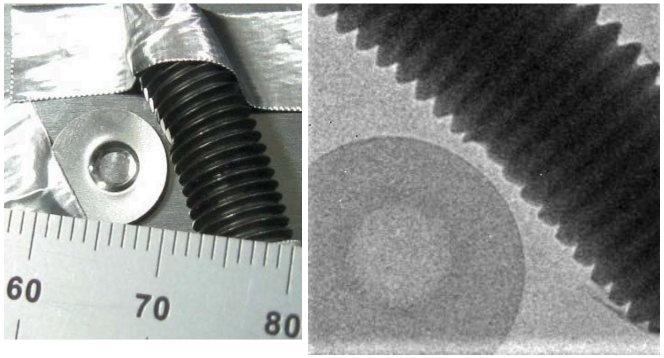

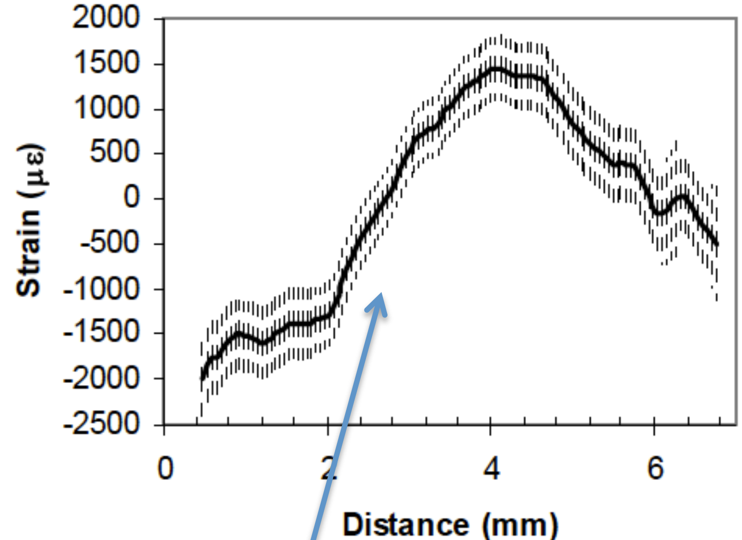

5 min exposure, 1 μs time res.

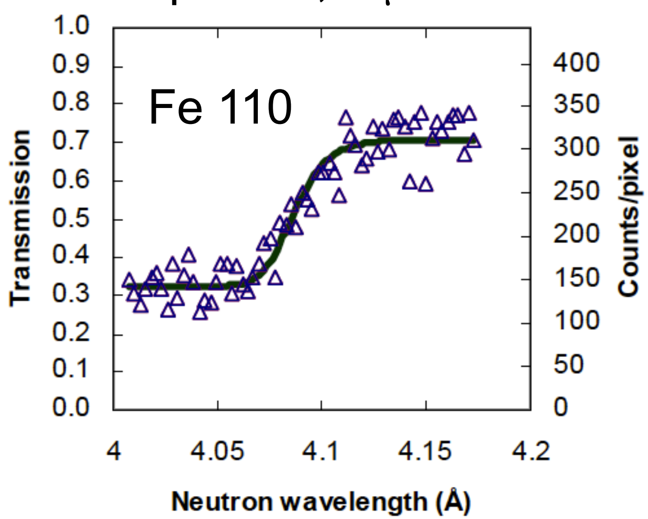

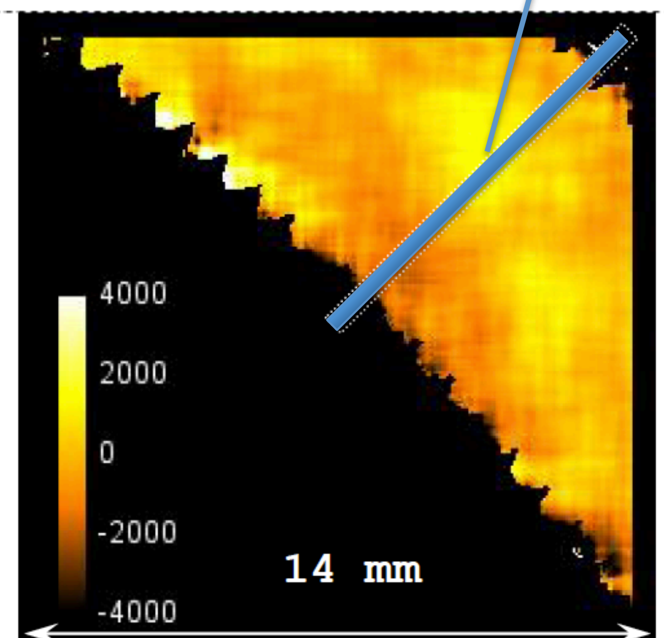

Strain map image of the steel screw. Strain values in μstrain

Tremsin et al., Journal of Physics, Conference Series 251 (2010) 012069

Bragg Edge Imaging

- **Texture mapping**

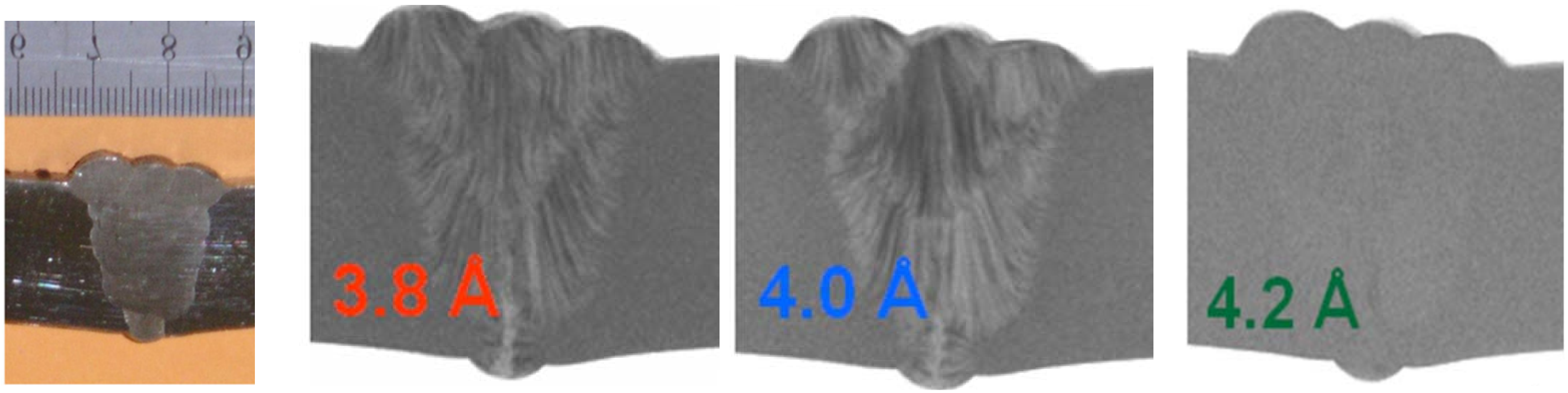

Bragg reflected neutrons result in narrow dips in the actual transmission at precise wavelengths specified by Bragg's law:

$$\lambda_{hkl} = 2d_{hkl} \sin\theta_{hkl}$$

where d_{hkl} is the interplanar distance for the (*hkl*) planes and θ_{hkl} are the Bragg angles θ_{hkl} depends on the relative orientation of the crystal lattice to the neutron beam.

At λ_{hkl}, creation of map of the number of crystals having any of their (*hkl*) directions making an angle, β_{hkl}, with the incident beam given by:

$$\beta_{hkl} = (\pi/2) - \arcsin(\lambda_{hkl} / 2d_{hkl})$$

Kockelmann et al., NIM A, Vol. 578 (2007) 421.

Propagation-based Neutron Phase Imaging

- Source needs to be spatially coherent (i.e. small pinhole and long pinhole-detector distances)
- Flux is low (up to 98% of flux is sacrificed, several hours to days for one radiograph)

D < 1 mm
L > 15 m

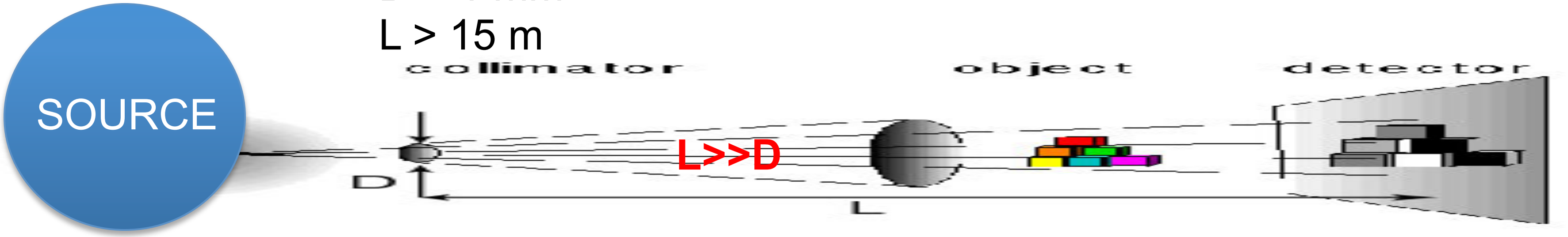

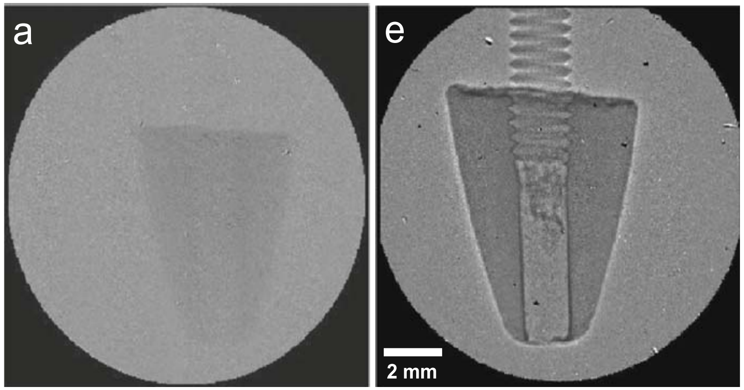

*(a) Neutron attenuation radiograph (e) and phase contrast radiograph of a lead sinker mounted on an Al screw. [B. Schillinger et al., **Mat. Trans. Proc.** (2006) 61]*

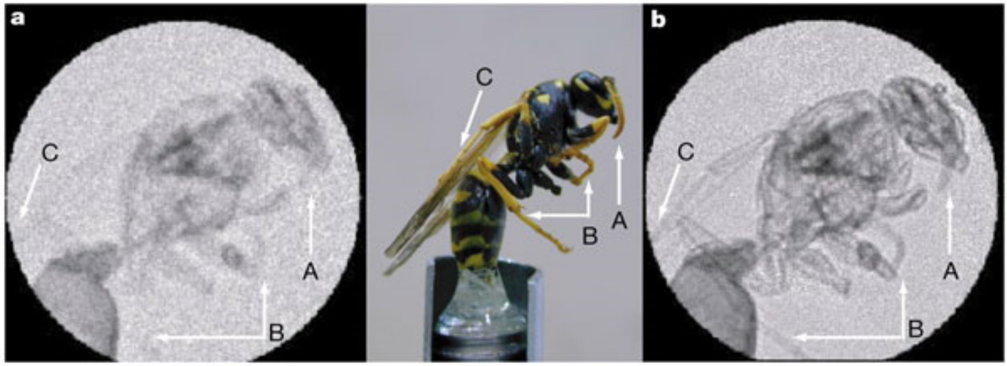

(a) Neutron attenuation radiograph (b) photograph and (c) phase contrast radiograph of a yellow jacket wasp.
*[B. E. Allman et al., **Nature** 408 (2000) 158]*

Phase Radiography using Grating Interferometry

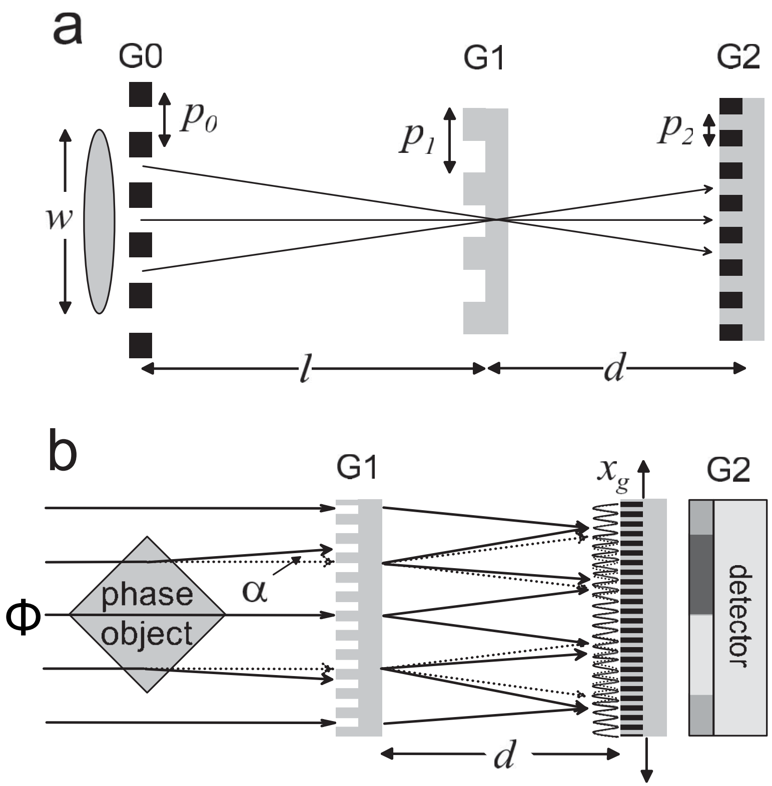

G0: (source) absorption grating, period p_0
G1: phase grating, period p_1
G2: (analyzer) absorption grating, period p_2

*[Pfeiffer et al., **PRL. 96** (2006) 215505]*

- G0 creates array of coherent sources from source *w*
- G1 creates diffraction patterns for each source which overlap if

$$p_0 = p_2 \frac{l}{d}$$

- Diffraction pattern has maximum contrast when *d* is a integer multiple of the Talbot length, L_T

$$L_T = \frac{p_1^2}{\lambda}$$

- Phase object cause distortion of diffraction pattern (or phase shift of incident wave Φ)
- Measure diffraction pattern by translating G2

$p_0 \sim 1$ mm, $p_1 \sim 10$ μm, $p_2 \sim 5$ μ m, $l \sim 5$ m, $d \sim 20$ mm

Stroboscopic imaging

- Makes a cyclically moving object appear to be slow moving
- Pulsed sources are by definition stroboscopic neutron sources

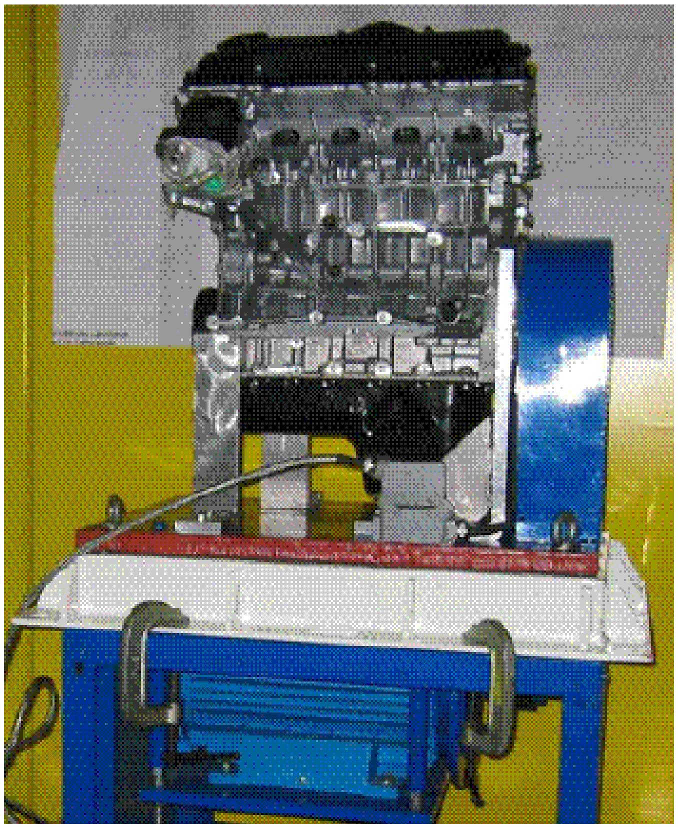

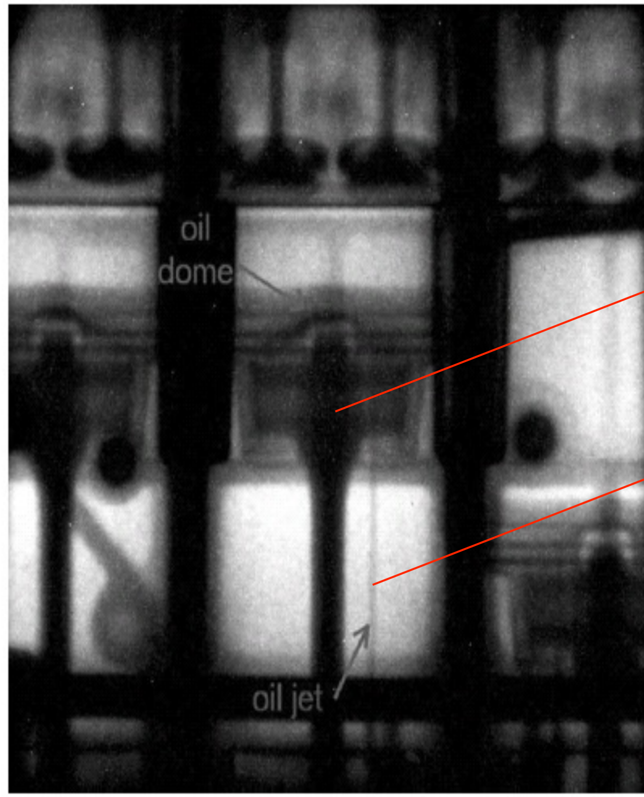

Oil spreading into bottom of piston

Oil jet ejected into bottom of piston

Stroboscopic imaging: 150 exposures, 200 ms each, 24 cm x 24 cm field of view

BMW engine, NEUTROGRAPH, ILL, France

Schillinger et al., NIM A **542** (2005) 142.

Applications at a glance

- Archeology
- Bio-medical
- Botany
- Contraband
- Cultural Heritage
- Energy
- Engineering/Materials Science
- Forensic Science
- Geology/Earth Sciences
- Homeland Security
- Paleontology
- Quality Assurance

Visualization of water transport in artificial soil sedimentation (20 s frame, 25 x 25 cm^2)

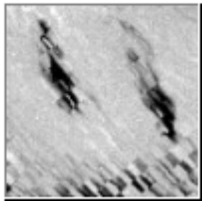

http://neutra.web.psi.ch/gallery/animations.html

Radiography of a dry monkey skull

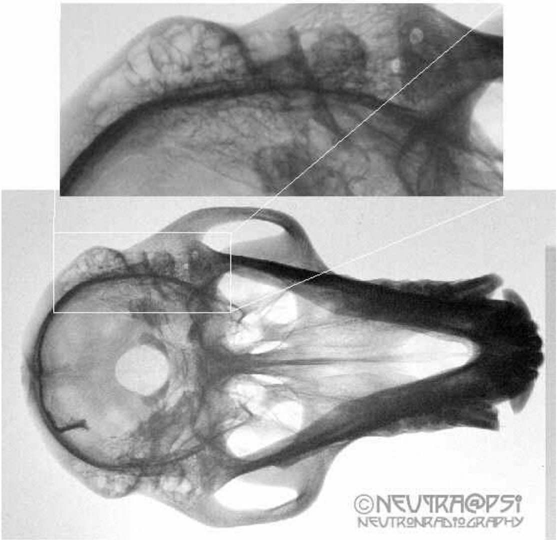

http://neutra.web.psi.ch/gallery/biological.html

Comparison of Li Distribution as a function of <u>depth</u> of battery

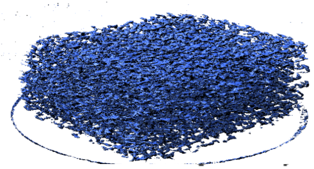

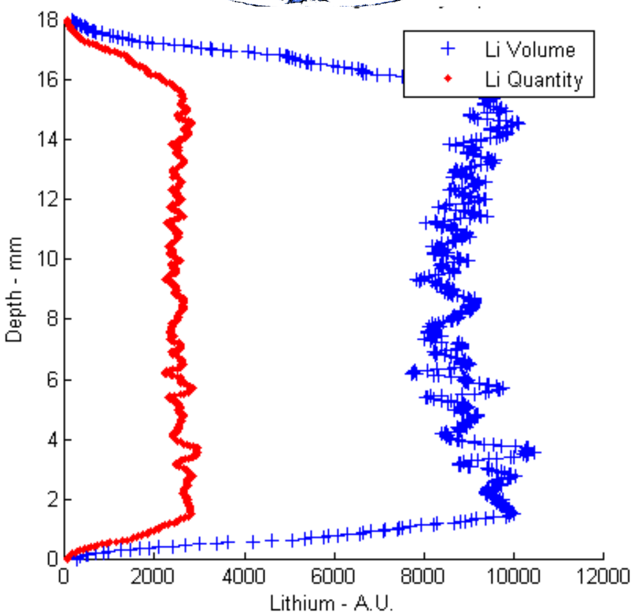

Control

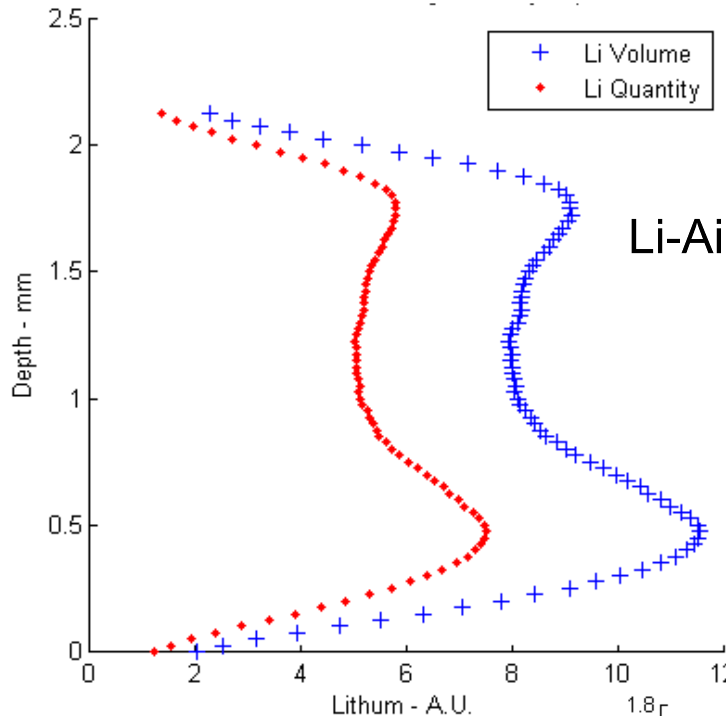

Li-Air (no catalyst)

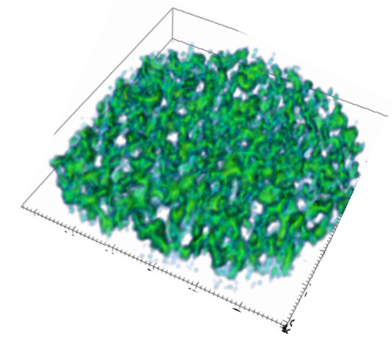

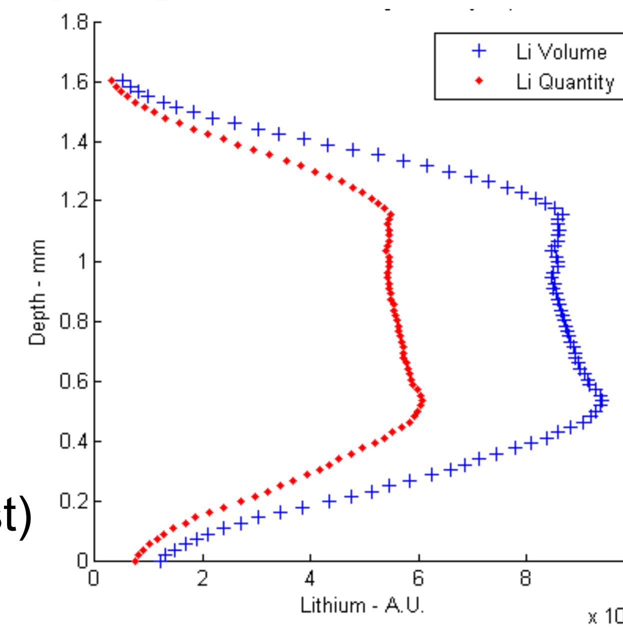

Li-Air (with catalyst)

Nanda et al., Journal of Physical Chemistry C, 2012.

Neutron Imaging Provides the Basis for Developing Models

Non-uniform lithium distribution may limit rechargeability

Neutron image
Li- air cathode

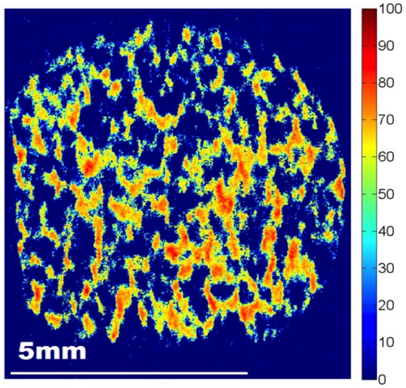

3D model
Li-air cathode

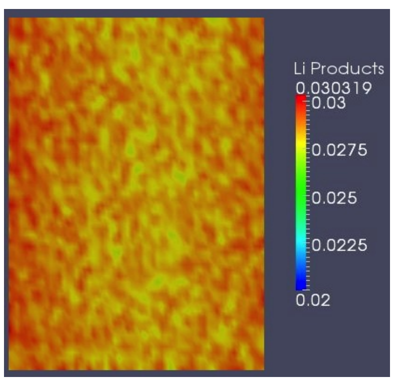

- **Reaction phase 3 dimensional modeling was used to predict results and compare with measurements**
- **Spatiotemporal reaction phase three-dimensional modeling of the electrodes also predicted a non-uniform lithium product distribution, confirming the neutron imaging result.**
- **Need to match resolution of neutron imaging capabilities to further improve feedback to modeling tools**

THE JOURNAL OF PHYSICAL CHEMISTRY C

Article

pubs.acs.org/JPCC

Anomalous Discharge Product Distribution in Lithium-Air Cathodes

Jagjit Nanda,*,† Hassina Bilheux,*,‡ Sophie Voisin,‡ Gabriel M. Veith,† Richard Archibald,§ Lakeisha Walker,‡ Srikanth Allu,§ Nancy J. Dudney,† and Sreekanth Pannala*,§

†Materials Science and Technology Division, ‡Neutron Scattering Science Division, and §Computer Science and Mathematics Division, Oak Ridge National Laboratory, Oak Ridge, Tennessee 37831, United States

Oak Ridge National Laboratory

Neutron CT of Turbine Blades

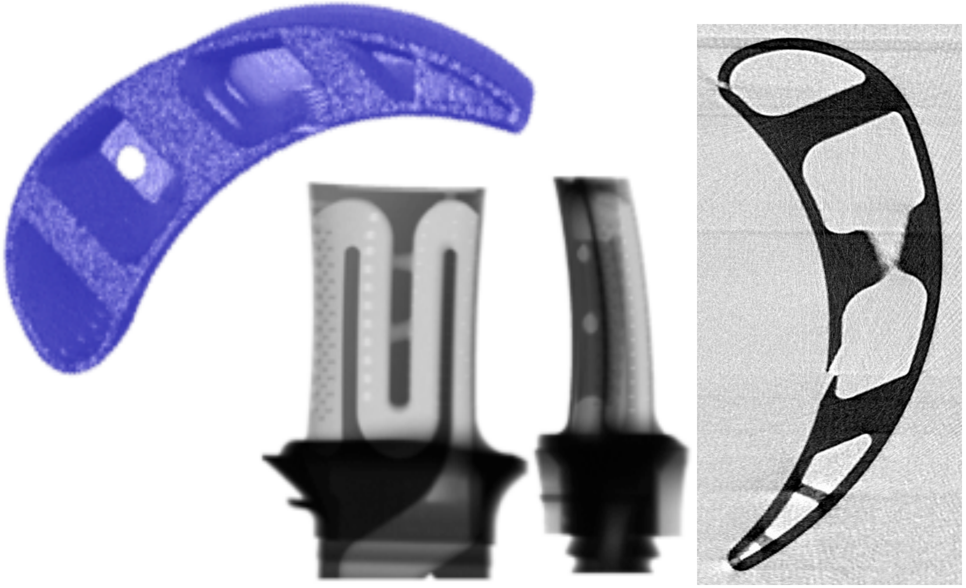

- **Comparison CAD engineering drawing and neutron computed tomographic data**
- **Porosity**
- **Surface roughness, cracks, defects**
- **In-situ cooling?**

T. Watkins, et al., *Advanced Materials and Processes*, March 2013.

Neutron Computed Tomography Characterizes Diesel Particulate Filter Regeneration Processes

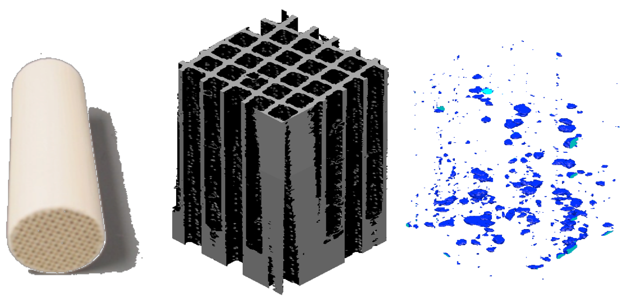

(1) Photograph, neutron tomography results showing a virtual separation of DPF walls (2) and particulate matter. (3) Soot cake density measured during sequential regeneration

T. J. Toops, H. Bilheux, S. Voisin, J. Gregor, L. Walker, A. Strzelec, C. E, A, Finney, J. A. Pihl, B. Schillinger, M. Schultz, Nuclear Instruments and Methods in Physics Research A, 2013.

Work performed at HFIR CG-1D Imaging Beamline

Scientific Achievement

Soot cake properties and distribution in sequentially regenerated diesel particulate filters (DPF) were assessed quantitatively using Neutron Computed Tomography (nCT) maps

Significance and Impact

Measured soot cake properties enable industry modelers and engine controllers to improved predictions and achieve more fuel-efficient regeneration

Research Details

- **Soot cake density, thickness and axial profile measured during sequential regeneration**
- **Different soot loading displayed same behavior during regeneration**
- **Highest soot cake density observed during initial 20% regeneration; afterwards porosity in the layer increases**
- **Quantitative findings directly relate to model parameters**

Ancient Craft Skills meet Modern Characterization

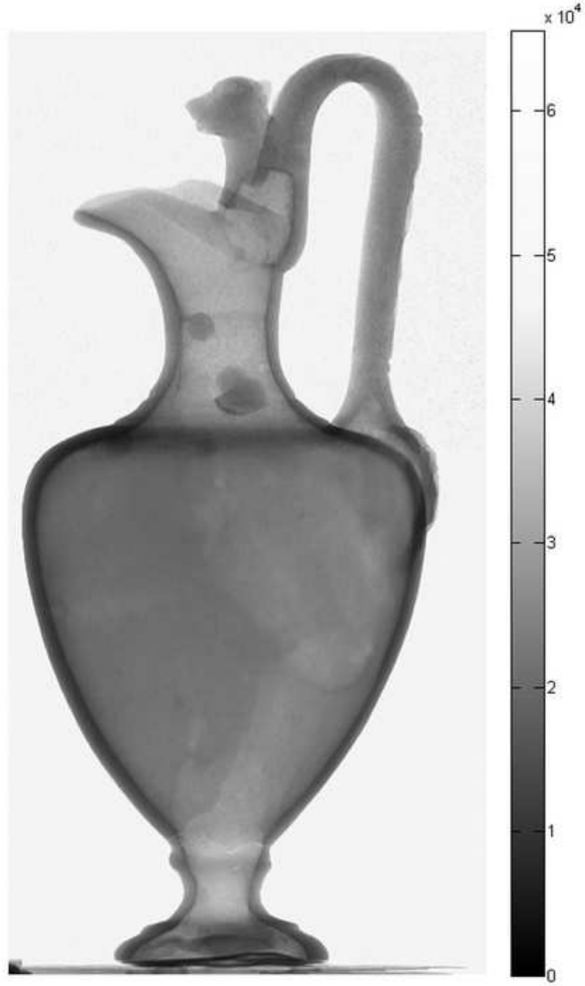

K. Ryzewski (PI), S. Herringer, H. Z. Bilheux, J.-C. Bilheux, B. Sheldon

Ancient Craft Skills meet Modern Characterization

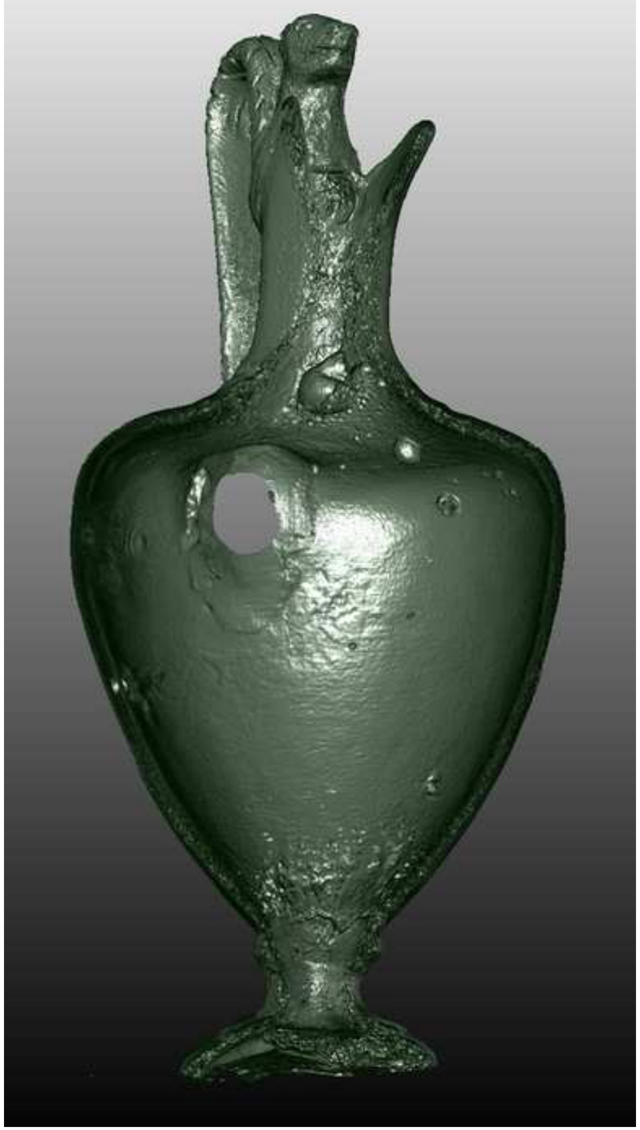

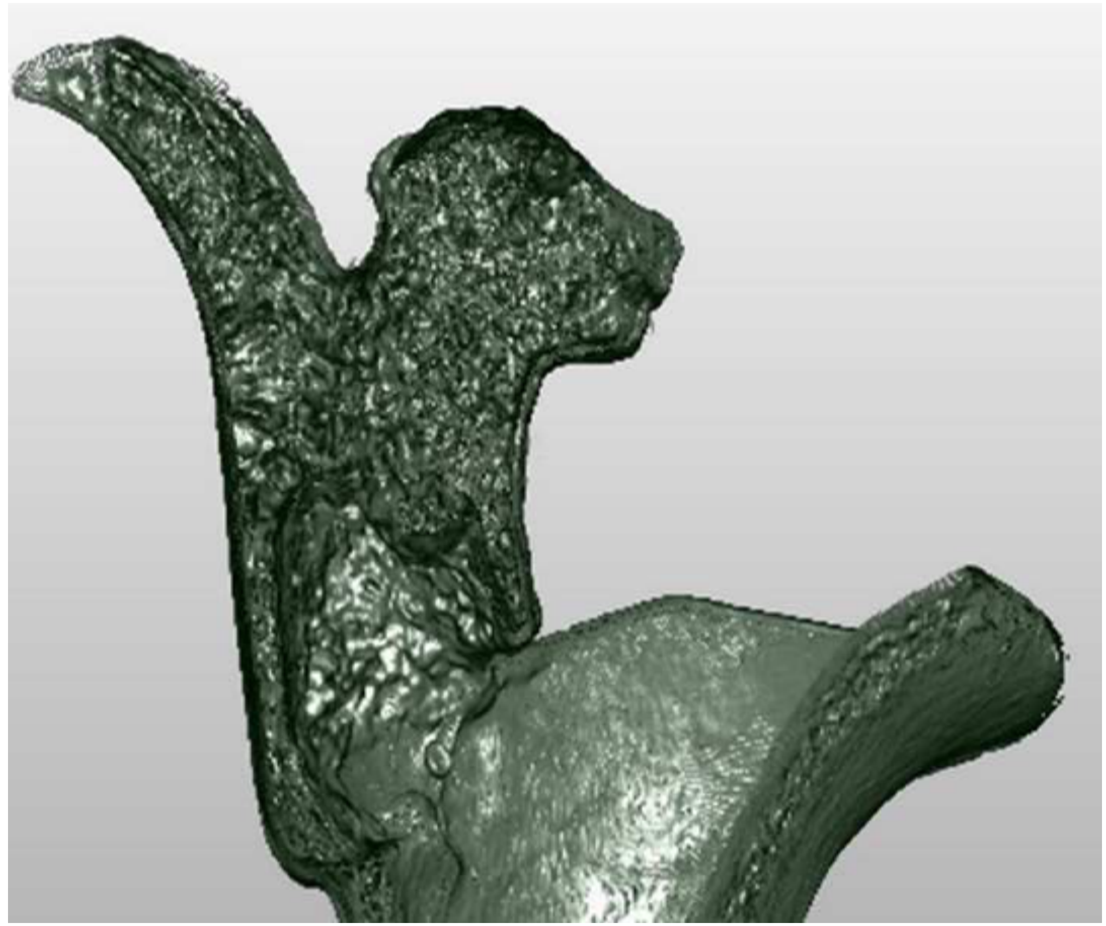

K. Ryzewski (PI), S. Herringer, H. Z. Bilheux, J.-C. Bilheux, B. Sheldon

Neutron Radiography of Roots at CG1-D

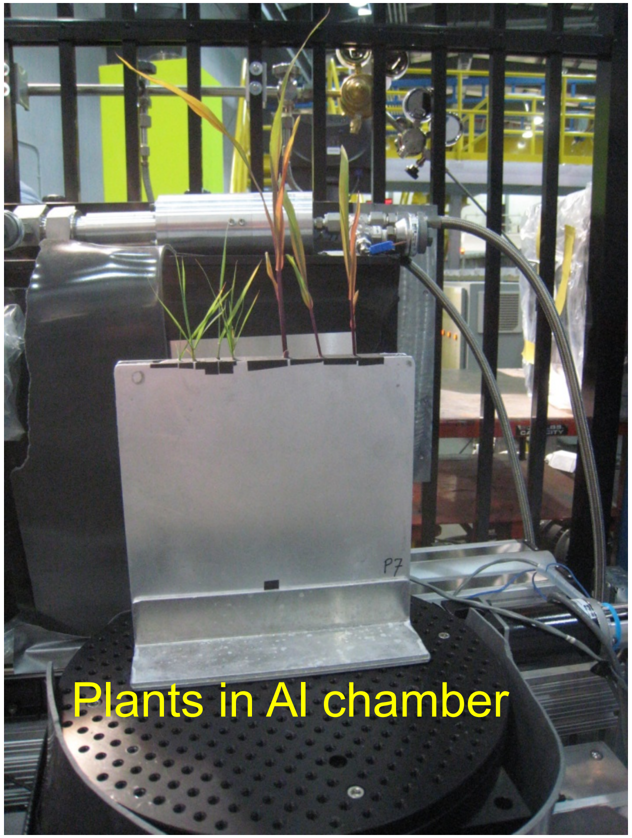

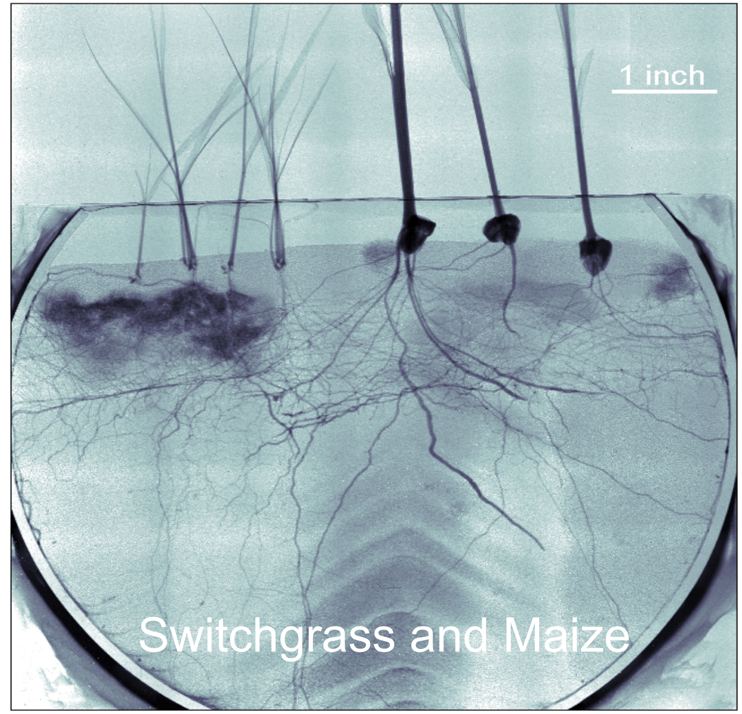

- Water injected into root zone at base
- Unidentified endophyte (symbiotic) or decomposer fungi visible near roots of switchgrass (left), revealing substantial hydration of the rhizosphere
- Both fine and coarse roots are readily visible

J. Warren (PI), H, Bilheux, M. Kang, S. Voisin, C. Cheng, J. Horita, E. Perfect, Plant Soil, 2013

Changes in Soil and Root Water Content using Neutron Radiography

t = 0 h t= 12 h t= 12/t= 0

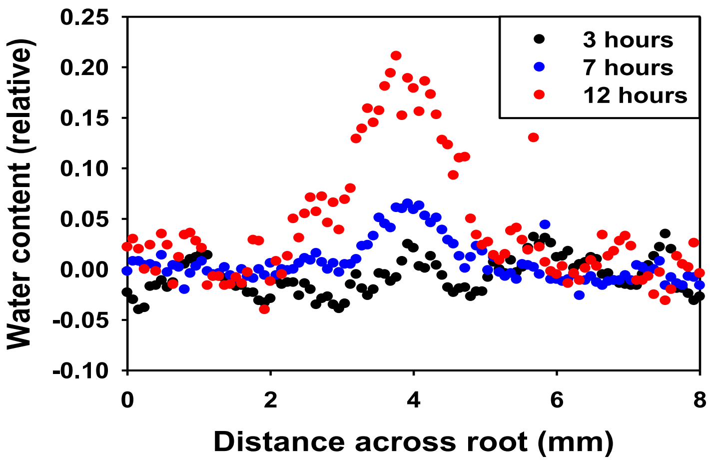

Top – More water showing up based on division (white areas)

Blue arrows show where water was removed from the system.

Left – increase in water content or root or rhizosphere due to root growth or root water efflux

J. Warren (PI), H, Bilheux, M. Kang, S. Voisin, C. Cheng, J. Horita, E. Perfect, Plant Soil, 2013

Water Uptake by Roots and Stem

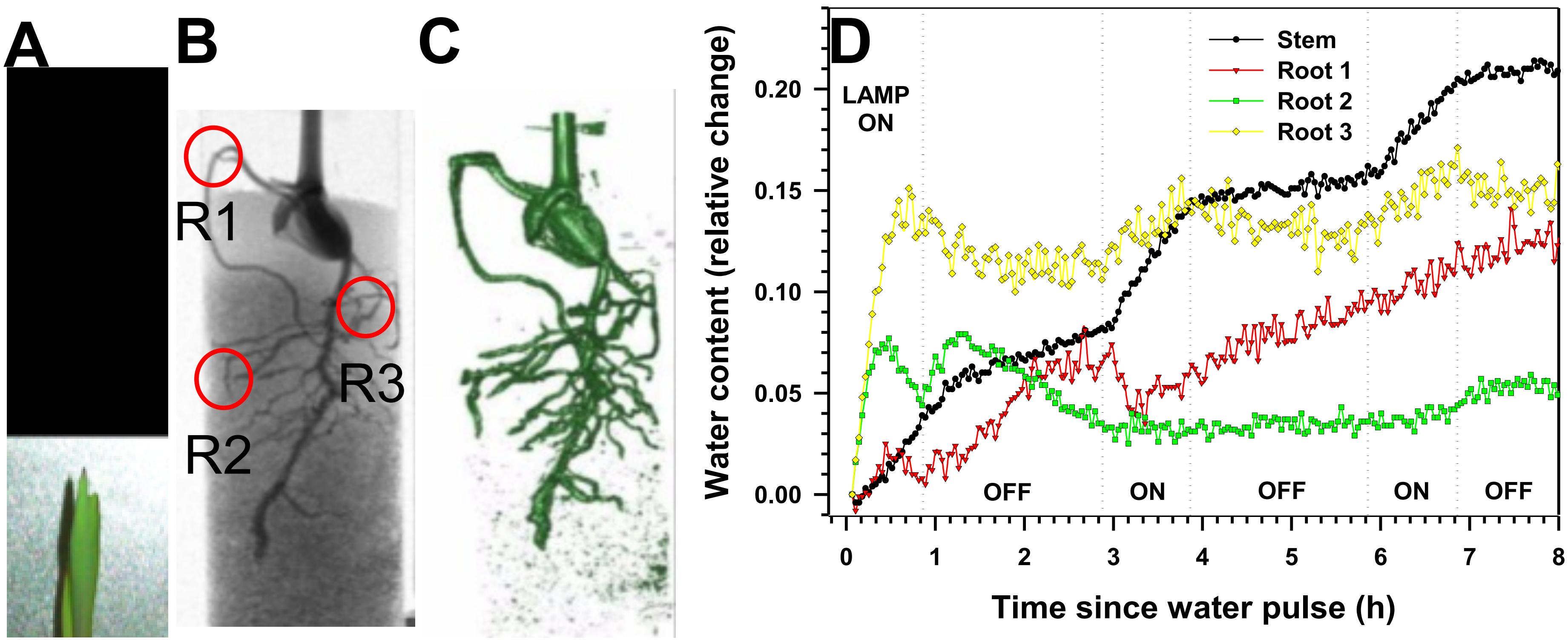

10-d old maize seedling (A) aluminum sample chamber; (B) neutron radiograph at ~70 µm pixel resolution illustrating roots distribution (0.2-1.6 mm); C) 3D tomographic reconstruction; (D) Timing of water uptake by plant components highlighted in (B) illustrating impact of solar radiation on rate of water flux in stem and ~0.5 mm first and second order roots.

➢ <u>This study provides direct evidence for root-mediated hydraulic redistribution of soil water to rehydrate drier roots</u>

J. Warren (PI), H. Bilheux, M. Kang, S. Voisin, C. Cheng, J. Horita, E. Perfect, Plant Soil, 2013

Thank you

(bilheuxhn@ornl.gov)

Courtesy of
Prof. Krysta Ryzewski, Wayne University
Susan Herringer, Prof. Brian Sheldon, Brown University